

Uplink Non-Orthogonal Multiple Access with Finite-Alphabet Inputs

Zheng Dong, He Chen, Jian-Kang Zhang, Lei Huang, and Branka Vucetic

Abstract

This paper focuses on the non-orthogonal multiple access (NOMA) design for a classical two-user multiple access channel (MAC) with finite-alphabet inputs. In contrast to most of existing NOMA designs using continuous Gaussian input distributions, we consider practical quadrature amplitude modulation (QAM) constellations at both transmitters, the sizes of which are assumed to be not necessarily identical. We propose to maximize the minimum Euclidean distance of the received sum-constellation with a maximum likelihood (ML) detector by adjusting the scaling factors (i.e., instantaneous transmitted powers and phases) of both users. The formulated problem is a *mixed continuous-discrete* optimization problem, which is nontrivial to resolve in general. By carefully observing the structure of the objective function, we discover that Farey sequence can be applied to tackle the formulated problem. However, the existing Farey sequence is not applicable when the constellation sizes of the two users are not the same. Motivated by this, we define a new type of Farey sequence, termed *punched Farey sequence*. Based on this, we manage to achieve a closed-form optimal solution to the original problem by first dividing the entire feasible region into a finite number of Farey intervals and then taking the maximum over all the possible intervals. The resulting sum-constellation is proved to be a regular QAM constellation of a larger size, and hence a simple quantization receiver can be implemented as the ML detector for the demodulation. Moreover, the superiority of NOMA over time-division multiple access (TDMA) in terms of minimum Euclidean distance is rigorously proved. Furthermore, the optimal rate allocation among the two users is obtained in closed-form to further maximize the obtained minimum Euclidean distance of the received signal subject to a total rate constraint. An asymptotic solution is also derived to reveal more insights on how to allocate the rate to each user. Finally, simulation results are provided to verify our theoretical analysis and demonstrate the merits of the proposed NOMA over existing orthogonal and non-orthogonal designs.

Z. Dong is with Shenzhen University, China and he is also with McMaster University, Canada (email: dongz3@mcmaster.ca), H. Chen and B. Vucetic are with The University of Sydney, Australia (email: {he.chen, branka.vucetic}@sydney.edu.au), J.-K. Zhang is with McMaster University, Canada (email: jkzhang@mail.ece.mcmaster.ca), Canada, and L. Huang is with Shenzhen University, China (email: lhuang8sasp@hotmail.com).

Index Terms

Non-orthogonal multiple access (NOMA), finite-alphabet inputs, multiple access channel (MAC), quadrature amplitude modulation (QAM), Farey sequence.

I. INTRODUCTION

The forthcoming fifth generation (5G) cellular systems are envisioned to support three generic services, including extreme mobile broadband (eMBB), massive machine-type communications (mMTC), and ultra-reliable and low-latency communications (uRLLC) [1], [2]. These diverse services, driven by the explosive growth of mobile data traffic and expected wide roll-out of Internet of Things (IoT), pose challenging requirements for the air interface of wireless networks where enhanced multiple access technologies are essential. Apart from several other potential technologies such as massive multiple-input multiple-output (MIMO) and millimeter wave (mmWave) communications, non-orthogonal multiple access (NOMA) has recently emerged as a key enabling radio access technology to meet these unprecedented requirements of 5G networks, due to its inherent advantages of high spectral efficiency, massive connectivity, and low transmission latency [3]–[7]. The concept of NOMA has multiple variants, such as power-domain NOMA, sparse code multiple access, pattern division multiple access, low density spreading, and lattice partition multiple access [5]. In this paper, we mainly consider the power-domain NOMA.

The basic principle of NOMA is to serve more than one user with distinct channel conditions simultaneously in the same orthogonal resource block along the time, frequency, or code axes. This can be achieved by applying the superposition coding (SC) at the transmitter as well as multiuser detector (e.g., successive interference cancellation (SIC)) at the receiver side to distinguish the co-channel users. As such, NOMA is fundamentally different from conventional orthogonal multiple access (OMA) methods primarily used in the previous generations of mobile systems, where each user is allocated to one dedicated orthogonal radio resource block exclusively. This in turn means that, in OMA, multiuser communication can be decomposed into several parallel single-user ones free of inter-user interference, and then the well-established single-user encoding/decoding methods can be directly applied with a reasonable tradeoff between network throughput and implementation complexity [8, Ch. 14].

Although the OMA schemes have been widely used in the past several decades, they generally cannot achieve the whole multiuser capacity region and thus tend to have a lower spectral efficiency than NOMA approaches [3], [5], [9], [10]. For example, in OMA, a resource block

allocated to a user with a poor channel condition cannot be reused by another user with a much stronger channel state. Apart from that, OMA is in general not scalable. This is because the amount of resource blocks as well as the granularity of user scheduling strictly limit the number of users that can be supported at the same time. On the contrary, by breaking the orthogonality of the radio resource allocation, NOMA has been shown to be able to provide better user fairness and improve physical layer security in addition to the advantages mentioned above [3], [5].

A. Related Work

Despite the fact that the deployment of NOMA as a new radio access technology in next-generation mobile systems is relatively new, the performance of NOMA has been studied extensively in the information theory society for various channel topologies such as broadcast channel (BC) [11]–[14], multiple access channel (MAC) [15]–[18], and interference channel (IC) [19]–[23]. However, these results concentrated mainly on the study of the channel capacity region with the assumption of unlimited encoding/decoding complexity, and therefore lie mostly in the theoretical aspects due to their extremely high implementation cost. Thanks to the rapid progress of the radio frequency (RF) chain and the processing capability of mobile devices in the past decades, the implementation of NOMA is becoming more and more feasible and thus has drawn tremendous attention from both academia and industry very recently [5]. More specifically, by taking practical constraints on user fairness and/or radio resource management into consideration, NOMA has been investigated in various wireless systems, such as cognitive radio [24], [25], cooperative communications [26], [27], cellular uplink [28], [29], cellular downlink [30]–[34], and multi-cell networks [35], [36]. In fact, a two-user downlink scenario of NOMA, known as multiuser superposition transmission (MUST), has already been incorporated in the 3rd Generation Partnership Project (3GPP) Long Term Evolution-Advanced (LTE-A) [37], [38].

We note that, up to now, the vast majority of existing NOMA designs assumed the use of Gaussian input signals [6], [11]–[16], [19]–[33], [35]. Although the Gaussian input is of great significance both theoretically and practically, its implementation in reality will require huge storage capacity, unaffordable computational complexity and extremely long decoding delay [9, Ch.9]. More importantly, the actual transmitted signals in real communication systems are drawn from finite-alphabet constellations, such as pulse amplitude modulation (PAM), quadrature amplitude modulation (QAM), and phase-shift keying (PSK) [8, Ch.5]. Applying the results

derived from the Gaussian inputs to the signals with finite-alphabet inputs can lead to significant performance loss [39]. In this sense, Gaussian input serves mostly as the theoretical benchmark.

Motivated by the above facts, the NOMA design with finite-alphabet inputs is of utmost importance and has attracted considerable efforts, see e.g., [36], [40]–[44] and references therein. The main principle¹ of these efforts is to ensure that the signal originated from each user can be uniquely decoded from the received sum-signal at the receiver side. By using mutual information as a performance measure, references [40], [41] considered the NOMA design in an ideal two-user Gaussian MAC with finite-input constellations under individual power constraint on each user. Specifically, NOMA was realized by strategically introducing certain constellation rotations (CR) to the adopted PSK signals in [40] or using proper power control in [41]. However, only numerical solutions to the optimal NOMA designs were provided in [40], [41]. Moreover, linear precoders were considered for the MIMO MAC in [42], where the expression of the weighted sum-rate was asymptotic and the optimal solution was also numerical. Besides, the downlink NOMA system with discrete input distributions was studied in [43], where the solution is intuitive based on the deterministic approximation of the actual fading channel. The discrete input alphabets were also considered for a two-user interference channel to evaluate the capacity inner bound in [44]. In other words, all NOMA designs provided in [40]–[44] used mutual information as the performance measure, where the solutions were numerical and limited insights on the relationship between the sum-constellation and each user’s constellation can thus be drawn from the obtained solutions.

B. Motivation and Contributions

Inspired by the aforementioned work, in this paper we target a *closed-form* NOMA design for a classical two-user Gaussian MAC with finite-alphabet inputs and an optimal maximum likelihood (ML) detector at the receiver, where the two users are allowed to transmit simultaneously in the same frequency band. Finding the capacity bound of a Gaussian MAC with Gaussian inputs and adaptive power control has always been a classic problem, see e.g., [15]–[18], [22], [23], [29], [48]; the optimal power control scheme for the Gaussian MAC with finite-alphabet inputs, however, is still an open problem and only numerical solutions are available [38], [40], [41], [49].

¹Note that the principle was originally proposed in the seminal work [45]–[47], wherein the finite-length codeword design problem in the binary domain were considered from an information-theoretical perspective.

To fill this gap, in this paper we, for the first time, investigate the optimal power control problem for the two-user Gaussian MAC with *finite square QAM constellations* that maximizes the minimum Euclidean distance of the received signals with the maximum likelihood (ML) detector. Note that QAM signaling is more spectrally efficient than other commonly-used constellations such as PSK signaling. Nevertheless, the NOMA design with QAM is more challenging than that with PSK since in QAM both the amplitude and the phase of the modulated signal vary, while in PSK only the phase is different, and thus the unambiguity of the sum-constellation at the receiver side is much more difficult to maintain. Here, it is worth pointing out that in our previous work [36], the NOMA design for the Gaussian Z-channel with QAM constellations was investigated, which incorporates the considered two-user MAC as a special case. In particular, to resolve the formulated problem, Farey sequence [50] was introduced to characterize the minimum Euclidean distance of the sum-constellation. However, due to the inherent symmetric structure between numerators and denominators of the conventional Farey sequence, our results presented in [36] refer to the case where both transmitters need to use an *identical* constellation size implying the same transmission rate. However, the transmission rates of the users are *not necessarily the same* in practice due to their distinct quality of service (QoS) requirements. To our best knowledge, the NOMA design in terms of power control at users for the Gaussian MAC with not necessarily identical QAM constellations still remains an open problem.

The main contributions of this paper can be summarized as follows:

- 1) We develop a practical NOMA design for the classical two-user complex Gaussian MAC, where the two users are allowed to adopt not necessarily the same QAM constellations. In our design framework, we aim to maximize the minimum Euclidean distance of the received sum-constellation at the receiver side, which dominates the error performance of the considered system, by adjusting the transmit power and phase of each user. To this end, we first decompose the complex MAC design problem into two real MAC design problems by strategically rotating the phase of the input signals at the two users. Nevertheless, the decomposed problems are still non-trivial due to their mixed continuous-and-discrete feature. Furthermore, our Farey sequence-based design framework developed in [36] can no longer be applied here due to the fact that the two users may use different QAM constellations.
- 2) To address this challenging problem, we define a new type of Farey sequence, termed *punched Farey sequence*, which is essential for our NOMA design with not necessarily

the same QAM constellations. This concept is even mathematically new to the best of our knowledge [50]. We identify and rigorously prove several important properties of the punched Farey sequence in parallel to the conventional Farey sequence. Based on the punched Farey sequence and its important properties, we manage to resolve the above decomposed problem for each channel branch by providing a neat closed-form optimal solution, which reveals that the optimal sum-constellation is a regular QAM constellation of a larger size. Due to this nice structure of the sum-constellation, a simple quantization decoder can be employed to implement the ML detector.

- 3) Based on the obtained closed-form solution, we prove the superiority of this NOMA design over the time-division multiple access (TDMA) approach in terms of the minimum Euclidean distance at the receiver for arbitrary given channel realization and rate allocation. Actually, this is a surprising result since the new NOMA method can achieve a better error performance than TDMA in a high SNR regime even if there is no near-far effect. Furthermore, we also address the optimal rate-allocation problem among the two users to maximize the minimum Euclidean distance of the received sum-constellation subject to a total rate constraint. More importantly, we derive a high-rate approximate solution to the optimal rate-allocation problem, which uncovers a lot of insights on the practical system designs.

II. TWO-USER GAUSSIAN MULTIPLE-ACCESS CHANNEL

We consider a two-user Gaussian MAC given by

$$z = h_1x_1 + h_2x_2 + \xi, \quad (1)$$

where z is the received signal at the base station (BS), h_k denotes the complex channel coefficient between the transmitter S_k and BS for $k = 1, 2$, and ξ is the additive zero-mean, circularly symmetric complex Gaussian (CSCG) noise with variance $2\sigma^2$, i.e., $\xi \sim \mathcal{CN}(0, 2\sigma^2)$. We assume that perfect channel state information (CSI) is available to all the nodes² and symbol synchronization is maintained at BS. The transmitted symbols x_k are superimposed at the receiver in a NOMA manner which are chosen randomly, independently and equally likely from the

²The optimal design can also be performed at the BS which sends the results back to the transmitters via the forward links. In this case, only BS needs to know the full CSI.

(finite) square QAM constellation \mathcal{Q}_k , and are subject to individual average power constraint P_k , i.e., $\mathbb{E}[|x_k|^2] \leq P_k$ for $k = 1, 2$.

Although we use a complex baseband representation in (1), the modulated and demodulated signals are real since the oscillator at the transmitter can only generate real sinusoids rather than complex exponentials, and the channel then introduces amplitude and phase distortion to the transmitted signals [8]. As such, we follow [41] to decompose the considered complex Gaussian MAC given in (1) into two parallel real-scalar Gaussian MACs, which are called the in-phase and quadrature components, respectively [8]. This means that the original two-dimensional QAM constellation can be split into two one-dimensional PAM constellations to be transmitted via the in-phase and quadrature branches. Besides, since the in-phase and quadrature components of the sum-constellation are separable, they can be decoded independently at the receiver, thereby reducing the decoding complexity. Mathematically, we notice that (1) is equivalent to

$$z = |h_1|x_1 \exp(j \arg(h_1)) + |h_2|x_2 \exp(j \arg(h_2)) + \xi. \quad (2)$$

To simplify the subsequent expressions, we let $y = \text{Re}(z)$, $y' = \text{Im}(z)$, $w_1 s_1 = \text{Re}(x_1 \exp(j \arg(h_1)))$, $w'_1 s'_1 = \text{Im}(x_1 \exp(j \arg(h_1)))$, $w_2 s_2 = \text{Re}(x_2 \exp(j \arg(h_2)))$, $w'_2 s'_2 = \text{Im}(x_2 \exp(j \arg(h_2)))$, $n = \text{Re}(\xi)$ and $n' = \text{Im}(\xi)$, where $\text{Re}(\cdot)$ and $\text{Im}(\cdot)$ are the real and imaginary parts of the complex number, respectively. Besides, w_1 , w_2 , w'_1 , and w'_2 are the real non-negative scalars determining the minimum Euclidean distance of the actual transmitted PAM constellation sets, which are referred to as the *weighting coefficients* throughout this paper. Now, the in-phase and quadrature branches of (1) can be reformulated by

$$y = |h_1|w_1 s_1 + |h_2|w_2 s_2 + n, \quad (3a)$$

$$y' = |h_1|w'_1 s'_1 + |h_2|w'_2 s'_2 + n', \quad (3b)$$

where $n, n' \sim \mathcal{N}(0, \sigma^2)$ are independent and identically distributed (i.i.d.) real additive white Gaussian components since the complex noise term ξ is assumed to be CSCG noise.

Without loss of generality, we assume that $x_1 \exp(j \arg(h_1)) \in \mathcal{Q}_1$ and $x_2 \exp(j \arg(h_2)) \in \mathcal{Q}_2$, where \mathcal{Q}_1 and \mathcal{Q}_2 are M_1^2 - and M_2^2 -ary square QAM constellations (M_1 and M_2 are both no less than 2 but not necessarily equal to each other), respectively, given by $\mathcal{Q}_1 \triangleq \{\pm w_1(2k - 1) \pm w'_1(2\ell - 1)j : k, \ell = 1, \dots, M_1/2\}$ and $\mathcal{Q}_2 \triangleq \{\pm w_2(2k - 1) \pm w'_2(2\ell - 1)j : k, \ell = 1, \dots, M_2/2\}$. As a result, the information-bearing symbols $s_1, s'_1 \in \mathcal{A}_{M_1} = \{\pm(2k - 1)\}_{k=1}^{M_1/2}$, sent by S_1 , and $s_2, s'_2 \in \mathcal{A}_{M_2} = \{\pm(2k - 1)\}_{k=1}^{M_2/2}$, transmitted by S_2 , are drawn from the

standard PAM constellations with equal probability. We consider that an equal power allocation between two branches is performed to balance the minimum Euclidean distance of the two PAM constellations [8, Ch. 6.1.4] and the transmitted signals over both subchannels should still be subject to average power constraints, i.e., $\mathbb{E}[w_1^2|s_1|^2] \leq P_1/2$, $\mathbb{E}[w_1'^2|s_1'|^2] \leq P_1/2$, $\mathbb{E}[w_2^2|s_2|^2] \leq P_2/2$, and $\mathbb{E}[w_2'^2|s_2'|^2] \leq P_2/2$.

An important problem for the considered MAC is, for any given QAM constellation sizes of both messages, how to optimize the values of scaling coefficients w_1 , w_2 , w_1' and w_2' to minimize the average error probability at the receiver, subject to the individual average power constraints at both transmitters. As the in-phase and quadrature subchannels are symmetric, if the same algorithm is applied to both branches, we will expect to have $w_1 = w_1'$ and $w_2 = w_2'$, and we call \mathcal{Q}_1 and \mathcal{Q}_2 the symmetric square QAM constellations. It is worth mentioning that our framework can be readily extended to un-symmetric signaling [51], [52], i.e., un-equal power allocation between the two branches. By leveraging the decomposable property of the complex Gaussian MAC and the symmetry of the two subchannels, we can simply focus on the design for one of the two real-scalar Gaussian MACs with PAM constellation sets, which will be elaborated in next section³.

III. THE WEIGHTING COEFFICIENTS DESIGN FOR THE REAL-SCALAR GAUSSIAN MAC

In this section, we consider the constellation design problem, i.e., finding the optimal weighting coefficients w_1 and w_2 , for the in-phase real-scalar Gaussian MAC. As the two sub-channels are symmetric, the optimal solution to the quadrature component can be obtained in exactly the same way and hence is omitted for brevity.

A. Problem Formulation

Recall that $\mathbb{E}[w_1^2|s_1|^2] \leq P_1/2$, $\mathbb{E}[w_2^2|s_2|^2] \leq P_2/2$, and hence $0 < w_1 \leq \sqrt{\frac{3P_1}{2(M_1^2-1)}}$, $0 < w_2 \leq \sqrt{\frac{3P_2}{2(M_2^2-1)}}$. For notation simplicity, we set $|\tilde{h}_1| = \sqrt{\frac{3P_1}{2(M_1^2-1)}}|h_1|$, $|\tilde{h}_2| = \sqrt{\frac{3P_2}{2(M_2^2-1)}}|h_2|$ and

$$\tilde{w}_1 = \sqrt{\frac{2(M_1^2-1)}{3P_1}}w_1, \tilde{w}_2 = \sqrt{\frac{2(M_2^2-1)}{3P_2}}w_2, \quad (4)$$

³It should be pointed out that designing two PAM constellations for both subchannels separately is a practical but not necessarily optimal approach. In fact, this approach has been widely adopted in literature, such as in [51]–[56]. How to design a two-dimensional complex constellation directly for the Gaussian MAC has been left as a future work.

where $0 < \tilde{w}_1 \leq 1$ and $0 < \tilde{w}_2 \leq 1$. The received signal in (3a) can thus be re-written as

$$y = |\tilde{h}_1|\tilde{w}_1s_1 + |\tilde{h}_2|\tilde{w}_2s_2 + n. \quad (5)$$

We assume that a coherent maximum-likelihood (ML) detector is used by BS to estimate the transmitted signals in a symbol-by-symbol fashion⁴. Mathematically, the estimated signals can be expressed as

$$(\hat{s}_1, \hat{s}_2) = \arg \min_{(s_1, s_2)} |y - (|\tilde{h}_1|\tilde{w}_1s_1 + |\tilde{h}_2|\tilde{w}_2s_2)|.$$

By applying the nearest neighbour approximation method [8, Ch.6.1.4] at high SNRs for ML receiver, the average error rate is dominated by the minimum Euclidean distance of the received constellation points owing to the exponential decaying of the Gaussian distribution. As such, in this paper, we aim to devise the optimal value of $(\tilde{w}_1, \tilde{w}_2)$ (or equivalently constellations \mathcal{Q}_1 and \mathcal{Q}_2) to maximize the minimum Euclidean distance of constellation points of the received signal. The Euclidean distance between the two received signals $y(s_1, s_2)$ and $y(\tilde{s}_1, \tilde{s}_2)$ at the receiver for (s_1, s_2) and $(\tilde{s}_1, \tilde{s}_2)$ in the noise-free case is given by

$$|y(s_1, s_2) - y(\tilde{s}_1, \tilde{s}_2)| = ||\tilde{h}_1|\tilde{w}_1(s_1 - \tilde{s}_1) - \tilde{h}_2|\tilde{w}_2(\tilde{s}_2 - s_2)||. \quad (6)$$

Note that s_1, \tilde{s}_1, s_2 and \tilde{s}_2 are all odd numbers, and thus we can let $s_1 - \tilde{s}_1 = 2n$ and $\tilde{s}_2 - s_2 = 2m$, in which $n \in \mathbb{Z}_{M_1-1}$ and $m \in \mathbb{Z}_{M_2-1}$ with $\mathbb{Z}_N \triangleq \{0, \pm 1, \dots, \pm N\}$ denoting the set containing all the possible differences. Similarly, we also define $\mathbb{Z}_{(M_1-1, M_2-1)}^2 \triangleq \{(a, b) : a \in \mathbb{Z}_{M_1-1}, b \in \mathbb{Z}_{M_2-1}\}$, and $\mathbb{N}_{(M_1-1, M_2-1)}^2 \triangleq \{(a, b) : a \in \mathbb{N}_{M_1-1}, b \in \mathbb{N}_{M_2-1}\}$ where $\mathbb{N}_N \triangleq \{0, 1, \dots, N\}$. From the definitions above, $(s_1, s_2) \neq (\tilde{s}_1, \tilde{s}_2)$ is equivalent to $(m, n) \neq (0, 0)$ (i.e., $m \neq 0$ or $n \neq 0$). To proceed, we define

$$\begin{aligned} d(m, n) &= \frac{1}{2}|y(s_1, s_2) - y(\tilde{s}_1, \tilde{s}_2)| \\ &= ||\tilde{h}_1|\tilde{w}_1n - \tilde{h}_2|\tilde{w}_2m||, \quad (m, n) \in \mathbb{Z}_{(M_1-1, M_2-1)}^2 \setminus \{(0, 0)\}, \end{aligned} \quad (7)$$

where $\mathcal{A} \setminus \mathcal{B} \triangleq \{x \in \mathcal{A} \text{ and } x \notin \mathcal{B}\}$. We are at a point to formally formulate the following max-min optimization problem,

⁴Since we perform a symbol-by-symbol detection, the decoding complexity is at most $\mathcal{O}(M_1M_2)$ with M_1 and M_2 being the PAM constellation size of s_1 and s_2 , respectively.

Problem 1: Power Control of NOMA in real-scalar MAC with PAM constellation: Find the optimal value of $(\tilde{w}_1^*, \tilde{w}_2^*)$ subject to the individual average power constraint such that the minimum Euclidean distance d^* of the received signal constellation points is maximized, i.e.,

$$(\tilde{w}_1^*, \tilde{w}_2^*) = \arg \max_{(\tilde{w}_1, \tilde{w}_2)} \min_{(m,n) \in \mathbb{Z}_{(M_1-1, M_2-1)}^2 \setminus \{(0,0)\}} d(m, n) \quad (8a)$$

$$\text{s.t. } 0 < \tilde{w}_1 \leq 1 \text{ and } 0 < \tilde{w}_2 \leq 1. \quad (8b)$$

■

Note that the inner optimization variable of finding the minimum Euclidean distances is discrete, while the outer one $(\tilde{w}_1, \tilde{w}_2)$ is continuous. In other words, Problem 1 is a *mixed continuous-discrete* optimization problem and it is in general hard to solve. To the best of our knowledge, only numerical solutions to such kind of problems are available in the open literature [38], [40], [41], [49]. To optimally and systematically solve this problem, we now develop a design framework based on the *Farey sequence* [50], in which the entire feasible region of $(\tilde{w}_1, \tilde{w}_2)$ is divided into a finite number of mutually exclusive sub-regions. Then, for each sub-region, the formulated optimization problem can be solved optimally with a closed-form solution, and subsequently the overall maximum value of Problem 1 can be attained by taking the maximum value of the objective function among all the possible sub-regions. We first consider the inner optimization problem in (8) given by:

Problem 2: Finding differential pairs with the minimum Euclidean distance:

$$\min_{(m,n) \in \mathbb{Z}_{(M_1-1, M_2-1)}^2 \setminus \{(0,0)\}} d(m, n) = \min_{(m,n) \in \mathbb{Z}_{(M_1-1, M_2-1)}^2 \setminus \{(0,0)\}} \left| |\tilde{h}_1| \tilde{w}_1 n - |\tilde{h}_2| \tilde{w}_2 m \right|. \quad (9)$$

■

We should point out that finding the closed-form solution to the optimal (m, n) for (9) is not trivial since the solution depends on the values of $|\tilde{h}_1|$ and $|\tilde{h}_2|$, which can span the whole positive real axis. Moreover, the values of \tilde{w}_1 and \tilde{w}_2 will be optimized later and cannot be determined beforehand. It is worth mentioning here that a similar optimization problem was formulated and resolved for a Gaussian Z channel in our previous work [36]. In [36], we resorted to the existing Farey sequence to solve the formulated problem. However, due to the inherent symmetric structure between numerators and denominators of the conventional Farey sequence, our results presented in [36] refers only to the case where both transmitters need to use exactly *identical* constellation size (i.e., the same transmission rate) and thus cannot be applied to the problem in this paper with M_1 and M_2 not necessarily the same. Motivated by this, in this paper we define

a new type of Farey sequence, termed punched Farey sequence. In the subsequent section, we will introduce the definition and some important properties of the original Farey sequence and the developed punched Farey sequence.

B. Farey Sequence

The Farey sequence characterizes the relationship between two positive integers and the formal definition is given as follows:

Definition 1: Farey sequence [50]: The Farey sequence \mathfrak{F}_K is the ascending sequence of irreducible fractions between 0 and 1 whose denominators are less than or equal to K . ■

By the definition, $\mathfrak{F}_K = \left(\frac{b_k}{a_k}\right)_{k=1}^{|\mathfrak{F}_K|}$ is a sequence of fractions $\frac{b_k}{a_k}$ such that $0 \leq b_k \leq a_k \leq K$ and $\langle a_k, b_k \rangle = 1$ arranged in an increasing order, where $\langle a, b \rangle$ denotes the largest common divider of non-negative integers a, b . In addition, $|\mathfrak{F}_K| = 1 + \sum_{m=1}^K \varphi(m)$ is the cardinality of \mathfrak{F}_K with $\varphi(\cdot)$ being the Euler's totient function [50]. An example of Farey sequence is given as follows:

Example 1: \mathfrak{F}_5 is the ordered sequence $\left(\frac{0}{1}, \frac{1}{5}, \frac{1}{4}, \frac{1}{3}, \frac{2}{5}, \frac{1}{2}, \frac{3}{5}, \frac{2}{3}, \frac{3}{4}, \frac{4}{5}, \frac{1}{1}\right)$.

It can be observed that each Farey sequence begins with number 0 (fraction $\frac{0}{1}$) and ends with 1 (fraction $\frac{1}{1}$). The series of breakpoints after $\frac{1}{1}$ is the reciprocal version of the Farey sequence. We call the Farey sequence together with its reciprocal version as the *extended Farey sequence* which is formally defined as follows:

Definition 2: Extended Farey sequence: The extended Farey sequence \mathfrak{S}_K of order K is the sequence of ascending irreducible fractions, where the maximum value of the numerator and denominator do not exceed K . ■

From the definition, we have $\mathfrak{S}_K = \left(\frac{b_k}{a_k}\right)_{k=1}^{|\mathfrak{S}_K|}$ with $\langle a_k, b_k \rangle = 1$ and $|\mathfrak{S}_K| = 1 + 2 \sum_{m=1}^K \varphi(m)$. We have the following example:

Example 2: \mathfrak{S}_5 is the sequence $\left(\frac{0}{1}, \frac{1}{5}, \frac{1}{4}, \frac{1}{3}, \frac{2}{5}, \frac{1}{2}, \frac{3}{5}, \frac{2}{3}, \frac{3}{4}, \frac{4}{5}, \frac{1}{1}, \frac{5}{4}, \frac{4}{3}, \frac{3}{2}, \frac{5}{3}, \frac{2}{1}, \frac{5}{2}, \frac{3}{1}, \frac{4}{1}, \frac{5}{1}, \frac{1}{0}\right)$.

It can be observed that the extended Farey sequence starts with number 0 (fraction $\frac{0}{1}$) and end with ∞ (fraction $\frac{1}{0}$). We now propose a new definition called *Punched Farey sequence* in number theory as follows.

Definition 3: Punched Farey sequence: The punched (extended) Farey sequence \mathfrak{P}_K^L is the ascending sequence of irreducible fractions whose denominators are no greater than K and numerators are no greater than L . ■

Example 3: \mathfrak{P}_5^2 is the ordered sequence $\left(\frac{0}{1}, \frac{1}{5}, \frac{1}{4}, \frac{1}{3}, \frac{2}{5}, \frac{1}{2}, \frac{2}{3}, \frac{1}{1}, \frac{2}{1}, \frac{1}{0}\right)$.

From Definition 3, when $L = K$, \mathfrak{P}_K^K degenerates into Farey sequence \mathfrak{F}_K , i.e., $\mathfrak{P}_K^K = \mathfrak{F}_K$. We can also observe that each punched Farey sequence begins with number 0 (fraction $\frac{0}{1}$) and ends with ∞ (fraction $\frac{1}{0}$).

We now develop some elementary properties of the punched Farey sequence in line with Farey sequences [50]. It is worth pointing out that, although for some properties, we can find the counterparts in conventional Farey sequences, the extension to the punched Farey sequences is non-trivial and the following results are new.

Property 1: If $\frac{n_1}{m_1}$ and $\frac{n_2}{m_2}$ are two adjacent terms (called Farey pairs) in \mathfrak{P}_K^L ($\min\{K, L\} \geq 2$) such that $\frac{n_1}{m_1} < \frac{n_2}{m_2}$, then, 1) $\frac{n_1+n_2}{m_1+m_2} \in (\frac{n_1}{m_1}, \frac{n_2}{m_2})$, $\frac{m_1+m_2}{n_1+n_2} \in (\frac{m_2}{n_2}, \frac{m_1}{n_1})$; 2) $m_1n_2 - m_2n_1 = 1$; 3) If $n_1 + n_2 \leq L$, then $m_1 + m_2 > K$ and if $m_1 + m_2 \leq K$, then $n_1 + n_2 > L$; 4) $n_1 + n_2 \geq 1$ where the equality is attained if and only if $\frac{n_1}{m_1} = \frac{0}{1}$ and $\frac{n_2}{m_2} = \frac{1}{K}$. Likewise, $m_1 + m_2 \geq 1$ where the equality is attained if and only if $\frac{n_1}{m_1} = \frac{L}{1}$ and $\frac{n_2}{m_2} = \frac{1}{0}$. ■

The proof is given in Appendix-A.

Property 2: If $\frac{n_1}{m_1}$, $\frac{n_2}{m_2}$ and $\frac{n_3}{m_3}$ are three consecutive terms in \mathfrak{P}_K^L with $\min\{K, L\} \geq 2$ such that $\frac{n_1}{m_1} < \frac{n_2}{m_2} < \frac{n_3}{m_3}$, then $\frac{n_2}{m_2} = \frac{n_1+n_3}{m_1+m_3}$. ■

The proof is provided in Appendix-B.

Property 3: Consider $\frac{n_1}{m_1}, \frac{n_2}{m_2}, \frac{n_3}{m_3}, \frac{n_4}{m_4} \in \mathfrak{P}_K^L$ with $\min\{K, L\} \geq 3$, such that $\frac{n_1}{m_1} < \frac{n_2}{m_2} < \frac{n_3}{m_3} < \frac{n_4}{m_4}$ where $\frac{n_2}{m_2}, \frac{n_3}{m_3}$ are successive in \mathfrak{P}_K^L , then $\frac{n_1+n_3}{m_1+m_3} \leq \frac{n_2}{m_2}$ and $\frac{n_3}{m_3} \leq \frac{n_2+n_4}{m_2+m_4}$. ■

The proof is provided in Appendix-C.

C. The Minimum Euclidean Distance of the Constellation Points of the Received Signal

We are now ready to solve Problem 2 to find the differential pairs (m, n) having the minimum Euclidean distance. To this end, we first introduce the following preliminary propositions.

Proposition 1: Let $\mathbb{F}_{(M_1-1, M_2-1)}^2 = \{(m, n) : \frac{n}{m} \in \mathfrak{P}_{M_2-1}^{M_1-1}\}$, and then

$$\min_{(m,n) \in \mathbb{Z}_{(M_1-1, M_2-1)}^2 \setminus \{(0,0)\}} d(m, n) = \min_{(m,n) \in \mathbb{F}_{(M_1-1, M_2-1)}^2} d(m, n). \quad \blacksquare$$

The proof is similar to [36, App.-A] and hence is omitted for brevity.

Proposition 2: Let $\frac{n_1}{m_1}$ and $\frac{n_2}{m_2}$ be two terms of $\mathfrak{P}_{M_2-1}^{M_1-1}$ such that $\frac{n_1}{m_1} < \frac{n_2}{m_2}$. Then, for $\frac{|\tilde{h}_2|\tilde{w}_2}{|\tilde{h}_1|\tilde{w}_1} \in (\frac{n_1}{m_1}, \frac{n_2}{m_2})$ and $d(m, n) = ||\tilde{h}_1|\tilde{w}_1n - |\tilde{h}_2|\tilde{w}_2m|$, we have 1) If $\frac{|\tilde{h}_2|\tilde{w}_2}{|\tilde{h}_1|\tilde{w}_1} = \frac{n_1+n_2}{m_1+m_2}$, then $d(m_1, n_1) = d(m_2, n_2)$; 2) If $\frac{|\tilde{h}_2|\tilde{w}_2}{|\tilde{h}_1|\tilde{w}_1} \in (\frac{n_1}{m_1}, \frac{n_1+n_2}{m_1+m_2})$, then $d(m_1, n_1) < d(m_2, n_2)$; 3) If $\frac{|\tilde{h}_2|\tilde{w}_2}{|\tilde{h}_1|\tilde{w}_1} \in (\frac{n_1+n_2}{m_1+m_2}, \frac{n_2}{m_2})$, then $d(m_2, n_2) < d(m_1, n_1)$. ■

The proof can be found in Appendix-D.

Proposition 3: For any $\frac{n_1}{m_1}, \frac{n_2}{m_2}, \frac{n_3}{m_3}, \frac{n_4}{m_4} \in \mathfrak{P}_{M_2-1}^{M_1-1}$ with $|\mathfrak{P}_{M_2-1}^{M_1-1}| \geq 4$, such that $\frac{n_1}{m_1} < \frac{n_2}{m_2} < \frac{n_3}{m_3} < \frac{n_4}{m_4}$, and $\frac{n_2}{m_2}, \frac{n_3}{m_3}$ are successive in $\mathfrak{P}_{M_2-1}^{M_1-1}$, we have 1) If $\frac{|\tilde{h}_2|\tilde{w}_2}{|\tilde{h}_1|\tilde{w}_1} \in (\frac{n_2}{m_2}, \frac{n_2+n_3}{m_2+m_3})$, then $\min_{(m,n) \in \mathbb{F}_{(M_1-1, M_2-1)}^2} d(m, n) = d(m_2, n_2) = |\tilde{h}_2|\tilde{w}_2 m_2 - |\tilde{h}_1|\tilde{w}_1 n_2$; 2) If $\frac{|\tilde{h}_2|\tilde{w}_2}{|\tilde{h}_1|\tilde{w}_1} \in (\frac{n_2+n_3}{m_2+m_3}, \frac{n_3}{m_3})$, then $\min_{(m,n) \in \mathbb{F}_{(M_1-1, M_2-1)}^2} d(m, n) = d(m_3, n_3) = |\tilde{h}_1|\tilde{w}_1 n_3 - |\tilde{h}_2|\tilde{w}_2 m_3$. ■

The proof is given in Appendix-E.

D. Closed-Form Optimal Solution to Problem 1

With the propositions presented in the previous subsection, we now can solve Problem 1 by restricting $\frac{|\tilde{h}_2|\tilde{w}_2}{|\tilde{h}_1|\tilde{w}_1}$ into a certain punched Farey interval determined by the corresponding Farey pair where a closed-form solution is attainable. More specifically, we consider the punched Farey sequence given by $\mathfrak{P}_{M_2-1}^{M_1-1} = (\frac{b_1}{a_1}, \frac{b_2}{a_2}, \dots, \frac{b_C}{a_C})$, where $C = |\mathfrak{P}_{M_2-1}^{M_1-1}|$. Now, assume that $\frac{|\tilde{h}_2|\tilde{w}_2}{|\tilde{h}_1|\tilde{w}_1} \in (\frac{b_k}{a_k}, \frac{b_{k+1}}{a_{k+1}})$ where $(\frac{b_k}{a_k}, \frac{b_{k+1}}{a_{k+1}})$ is the k -th punched Farey interval for $k = 1, \dots, C-1$, and we aim to find the optimal $(\tilde{w}_1^*(k), \tilde{w}_2^*(k))$ such that

$$g\left(\frac{b_k}{a_k}, \frac{b_{k+1}}{a_{k+1}}\right) = \max_{(\tilde{w}_1, \tilde{w}_2)} \min_{(m,n) \in \mathbb{F}_{(M_1-1, M_2-1)}^2} d(m, n) \quad (10a)$$

$$\text{s.t. } \frac{b_k}{a_k} < \frac{|\tilde{h}_2|\tilde{w}_2}{|\tilde{h}_1|\tilde{w}_1} \leq \frac{b_{k+1}}{a_{k+1}}, 0 < \tilde{w}_1 \leq 1 \text{ and } 0 < \tilde{w}_2 \leq 1. \quad (10b)$$

By applying the propositions in last subsections, we obtained the following lemma related to the optimal solution to problem (10).

Lemma 1: The optimal solution to (10) is given as follows:

$$g\left(\frac{b_k}{a_k}, \frac{b_{k+1}}{a_{k+1}}\right) = \begin{cases} \frac{|\tilde{h}_2|}{b_k + b_{k+1}}, & \text{with } (\tilde{w}_1^*(k), \tilde{w}_2^*(k)) = \left(\frac{|\tilde{h}_2|(a_k + a_{k+1})}{|\tilde{h}_1|(b_k + b_{k+1})}, 1\right), & \text{if } \frac{|\tilde{h}_2|}{|\tilde{h}_1|} \leq \frac{b_k + b_{k+1}}{a_k + a_{k+1}}; \\ \frac{|\tilde{h}_1|}{a_k + a_{k+1}}, & \text{with } (\tilde{w}_1^*(k), \tilde{w}_2^*(k)) = \left(1, \frac{|\tilde{h}_1|(b_k + b_{k+1})}{|\tilde{h}_2|(a_k + a_{k+1})}\right), & \text{if } \frac{|\tilde{h}_2|}{|\tilde{h}_1|} > \frac{b_k + b_{k+1}}{a_k + a_{k+1}}. \end{cases}$$

The proof of Lemma 1 can be found in Appendix-F.

Now, we are ready to present the closed-form optimal solution to Problem 1 in terms of (w_1^*, w_2^*) instead of $(\tilde{w}_1^*, \tilde{w}_2^*)$ defined in (4) for clarity, which maximizes the minimum Euclidean distance of the sum-constellation, denoted by d_{noMA} , over the entire feasible region.

Theorem 1: Closed-form optimal weighting coefficients: The optimal solution to Problem 1 in terms of (w_1^*, w_2^*) is given by:

$$(w_1^*, w_2^*) = \begin{cases} \left(\sqrt{\frac{3P_2 M_2^2}{2(M_2^2-1)}} \frac{|h_2|}{|h_1|}, \sqrt{\frac{3P_2}{2(M_2^2-1)}} \right), & \text{if } \frac{|h_2|}{|h_1|} \leq \sqrt{\frac{P_1(M_2^2-1)}{P_2 M_2^2(M_1^2-1)}}; \\ \left(\sqrt{\frac{3P_1}{2(M_1^2-1)}}, \sqrt{\frac{3P_1}{2M_2^2(M_1^2-1)}} \frac{|h_1|}{|h_2|} \right), & \text{if } \sqrt{\frac{P_1(M_2^2-1)}{P_2 M_2^2(M_1^2-1)}} < \frac{|h_2|}{|h_1|} \leq \sqrt{\frac{P_1 M_1^2(M_2^2-1)}{P_2 M_2^2(M_1^2-1)}}; \\ \left(\sqrt{\frac{3P_2}{2M_1^2(M_2^2-1)}} \frac{|h_2|}{|h_1|}, \sqrt{\frac{3P_2}{2(M_2^2-1)}} \right), & \text{if } \sqrt{\frac{P_1 M_1^2(M_2^2-1)}{P_2 M_2^2(M_1^2-1)}} < \frac{|h_2|}{|h_1|} \leq \sqrt{\frac{P_1 M_1^2(M_2^2-1)}{P_2(M_1^2-1)}}; \\ \left(\sqrt{\frac{3P_1}{2(M_1^2-1)}}, \sqrt{\frac{3P_1 M_1^2}{2(M_1^2-1)}} \frac{|h_1|}{|h_2|} \right), & \text{if } \sqrt{\frac{P_1 M_1^2(M_2^2-1)}{P_2(M_1^2-1)}} < \frac{|h_2|}{|h_1|}. \end{cases} \quad (11)$$

The resulting minimum Euclidean distance d_{nomia} in each case is:

$$d_{\text{nomia}} = \begin{cases} \sqrt{\frac{3P_2}{2(M_2^2-1)}} |h_2|, & \text{if } \frac{|h_2|}{|h_1|} \leq \sqrt{\frac{P_1(M_2^2-1)}{P_2 M_2^2(M_1^2-1)}}; \\ \sqrt{\frac{3P_1}{2M_2^2(M_1^2-1)}} |h_1|, & \text{if } \sqrt{\frac{P_1(M_2^2-1)}{P_2 M_2^2(M_1^2-1)}} < \frac{|h_2|}{|h_1|} \leq \sqrt{\frac{P_1 M_1^2(M_2^2-1)}{P_2 M_2^2(M_1^2-1)}}; \\ \sqrt{\frac{3P_2}{2M_1^2(M_2^2-1)}} |h_2|, & \text{if } \sqrt{\frac{P_1 M_1^2(M_2^2-1)}{P_2 M_2^2(M_1^2-1)}} < \frac{|h_2|}{|h_1|} \leq \sqrt{\frac{P_1 M_1^2(M_2^2-1)}{P_2(M_1^2-1)}}; \\ \sqrt{\frac{3P_1}{2(M_1^2-1)}} |h_1|, & \text{if } \sqrt{\frac{P_1 M_1^2(M_2^2-1)}{P_2(M_1^2-1)}} < \frac{|h_2|}{|h_1|}. \end{cases} \quad (12)$$

The proof is provided in Appendix-G. ■

Remark 1: By combing Eqs. (4) and (11), we can observe that at least one transmitter should transmit with the maximum power. The principle behind this is that we could always scale up both users' transmit powers without violating the power constraint such that the minimum Euclidean distance is enlarged. ■

We have the following remark regarding the choice of constellation size M_1, M_2 .

Remark 2: In order to attain the results in Theorem 1 with the aid of Farey sequence, we assume that $\min\{M_1, M_2\} \geq 2$. However, it can be verified that for $M_1 = 1, M_2 \geq 2$ or $M_1 \geq 2, M_2 = 1$, although (11) is no longer true, (12) still holds. In fact, if $M_1 = 1, M_2 \geq 2$, we have $(w_1^*, w_2^*) = (0, \sqrt{\frac{3P_2}{2(M_2^2-1)}})$. Else if $M_1 \geq 2, M_2 = 1$, we have $(w_1^*, w_2^*) = (\sqrt{\frac{3P_1}{2(M_1^2-1)}}, 0)$. That is, by assuming $M_k = 1, k = 1, 2$, i.e., no information is transmitted by user S_k , we should let it keep silent, and thus all the channel resources are allocated to the other user exclusively, who should transmit at its maximum allowable power. ■

We also have the following corollary about the optimal solution described in Theorem 1:

Corollary 1: The sum-constellation at the receiver is a *standard* $M_1^2 M_2^2$ -QAM constellation with the minimum Euclidean distance d_{nomia} affected by the instantaneous channel realizations as given in (12). ■

The proof is provided in Appendix-H.

Due to this nice structure of the sum-constellation, the ML decoder reduces to a simple quantizer for the complex constellation [34], where the detection can be performed for the in-phase and quadrature components separately since they are separable. It is worth mentioning that if $\frac{|h_2|}{|h_1|} \leq \sqrt{\frac{P_1 M_1^2 (M_2^2 - 1)}{P_2 M_2^2 (M_1^2 - 1)}}$, we have $\frac{|h_1| w_1^*}{|h_2| w_2^*} = M_2$, i.e., the constellation of S_2 will have a smaller Euclidean distance than that of S_1 at the receiver side; Otherwise if $\frac{|h_2|}{|h_1|} > \sqrt{\frac{P_1 M_1^2 (M_2^2 - 1)}{P_2 M_2^2 (M_1^2 - 1)}}$, we attain $\frac{|h_1| w_1^*}{|h_2| w_2^*} = \frac{1}{M_1}$, i.e., the constellation of S_1 will have a smaller Euclidean distance than that of S_2 .

E. The Superiority of NOMA over TDMA

It is significant to conduct comparisons between NOMA and OMA, such as in [57]. Now, to facilitate this comparison of NOMA over OMA with finite-alphabet inputs, we compare the minimum Euclidean distance of the proposed NOMA and that of TDMA under the same channel realization. In general, for TDMA, the overall available frame is partitioned *uniformly* into orthogonal time slots of the same length for the ease of symbol synchronization. Specifically, for a two-user TDMA, we assume that each user has half of the total available time slots and therefore, they should employ M_1^2 - and M_2^2 -ary PAM constellations, respectively, to maintain the same transmission rate. In this comparison, we also assume that the channel state of both users remains unchanged (i.e., quasi-static) during the two consecutive time slots.

For TDMA, the minimum Euclidean distance for users S_1 and S_2 are $d_{\text{oma},1} = \sqrt{\frac{3P_1}{2(M_1^4 - 1)}} |h_1|$ and $d_{\text{oma},2} = \sqrt{\frac{3P_2}{2(M_2^4 - 1)}} |h_2|$, respectively. Now, we denote the minimum Euclidean distance among the two users as:

$$d_{\text{oma}} = \min \{d_{\text{oma},1}, d_{\text{oma},2}\} = \min \left\{ \sqrt{\frac{3P_1}{2(M_1^4 - 1)}} |h_1|, \sqrt{\frac{3P_2}{2(M_2^4 - 1)}} |h_2| \right\}. \quad (13)$$

We then have the following corollary regarding the resulting minimum Euclidean distance of both schemes:

Corollary 2: The minimum Euclidean distance of the proposed NOMA, d_{noma} given in (12), is strictly larger than that of the TDMA scheme, d_{oma} given in (13), with equal time-slot allocation. That is, $d_{\text{noma}} > d_{\text{oma}}$ holds for arbitrary given channel realizations h_1, h_2 and constellation sizes M_1, M_2 . ■

The proof is provided in Appendix-I. From Corollary 2, since $d_{\text{noma}} > d_{\text{oma}}$, it is expected that NOMA outperforms TDMA in terms of error performance, especially in moderate and high SNR regions as can be confirmed by numerical results.

IV. RATE ALLOCATION IN TWO-USER GAUSSIAN MAC WITH SUM-RATE CONSTRAINT

In this section, we consider the optimal rate-allocation problem among the two users under a sum-rate constraint for the above two-user Gaussian MAC with a finite PAM constellation. Moreover, a high-rate asymptotically optimal solution is also provided when the transmission rates of both users are relatively high.

A. Problem Formulation

From a radio resource management perspective, when user fairness is not a major concern, one of the most important problems is to maximize the minimum Euclidean distance at the receiver side, which determines the system error performance in moderate and high SNR regimes. This motivates us to consider the maximization of d_{noma} in (12) under a sum-rate constraint. Mathematically speaking, we intend to solve the following optimization problem:

Problem 3: Rate allocation in two-user MAC under a sum-rate constraint: We aim to maximize the minimum Euclidean distance of the received sum-constellation d_{noma} given in (12) by adjusting the constellation sizes of both users under a sum-rate constraint, that is:

$$\max_{M_1, M_2} d_{\text{noma}} \quad \text{s.t.} \quad \log_2 M_1 + \log_2 M_2 = \log_2 M, \quad (14)$$

where M is the size of the sum-constellation, and $\log_2 M_1, \log_2 M_2 \in \mathbb{N}_{\log_2 M}$ (i.e., M_1, M_2 are non-negative integer powers of 2). ■

B. Optimal Rate Allocation

In this subsection, we investigate the above rate-allocation problem. From (14), we have $M_2 = M/M_1$, and therefore the minimum distance d_{noma} can be considered as a piecewise function of M_1 for any given $\lambda = \frac{P_2|h_2|^2}{P_1|h_1|^2}$. Note that, in (14), the channel coefficients $|h_1|, |h_2|$ and power constraints P_1, P_2 are treated as constant, and thus λ is also considered as a known

constant. Then, Problem 3 is equivalent to the minimization of $\beta(M_1) = \frac{3P_1|h_1|^2}{2d_{\text{noma}}^2}$ and with the help of (12), we can attain:

$$\beta(M_1) = \begin{cases} \frac{1}{\lambda} \left(\frac{M^2}{M_1^2} - 1 \right), & \text{if } 1 \leq M_1 \leq \gamma_1(\lambda); \\ M^2 - \frac{M^2}{M_1^2}, & \text{if } \gamma_1(\lambda) < M_1 \leq \gamma_2(\lambda); \\ \frac{1}{\lambda} (M^2 - M_1^2), & \text{if } \gamma_2(\lambda) < M_1 \leq \gamma_3(\lambda); \\ M_1^2 - 1, & \text{if } \gamma_3(\lambda) < M_1 \leq M, \end{cases} \quad (15)$$

where $\gamma_1(\lambda) = \sqrt{\frac{\lambda+1}{\lambda+\frac{1}{M^2}}}$, $\gamma_2(\lambda) = \sqrt{\frac{\sqrt{(\lambda-1)^2 + \frac{4\lambda}{M^2}} - (\lambda-1)}{2}} M$, and $\gamma_3(\lambda) = \sqrt{\frac{\lambda+M^2}{\lambda+1}}$.

From (15), we can find that, $\beta(M_1)$ is monotonically decreasing for $1 \leq M_1 \leq \gamma_1(\lambda)$ and $\gamma_2(\lambda) < M_1 \leq \gamma_3(\lambda)$, and it is monotonically increasing for $\gamma_1(\lambda) < M_1 \leq \gamma_2(\lambda)$ and $\gamma_3(\lambda) < M_1 \leq M$. Consequently, the optimal rate-allocation solution can be stated as follows:

Theorem 2: The optimal solution to Problem 3 is $M_1^* = M_{1,(k^*)}$ and $M_2^* = M/M_1^*$ such that $k^* = \arg \min \beta_k$, in which $\beta_1 = \frac{1}{\lambda} \left(\frac{M^2}{M_{1,(1)}^2} - 1 \right)$, where $M_{1,(1)} = 2^{\lfloor \log_2 \gamma_1(\lambda) \rfloor}$;

$$\beta_2 = \begin{cases} M^2 - \frac{M^2}{M_{1,(2)}^2}, & \text{if } \lfloor \log_2 \gamma_1(\lambda) \rfloor \leq \lfloor \log_2 \gamma_2(\lambda) \rfloor + 1 \\ \infty, & \text{otherwise} \end{cases}, \text{ where } M_{1,(2)} = 2^{\lfloor \log_2 \gamma_1(\lambda) \rfloor + 1};$$

$$\beta_3 = \begin{cases} \frac{1}{\lambda} (M^2 - M_{1,(3)}^2), & \text{if } \lfloor \log_2 \gamma_2(\lambda) \rfloor \leq \lfloor \log_2 \gamma_3(\lambda) \rfloor + 1 \\ \infty, & \text{otherwise} \end{cases}, \text{ where } M_{1,(3)} = 2^{\lfloor \log_2 \gamma_3(\lambda) \rfloor};$$

and $\beta_4 = M_{1,(4)}^2 - 1$, where $M_{1,(4)} = 2^{\lfloor \log_2 \gamma_3(\lambda) \rfloor + 1}$, where $\lfloor a \rfloor$ is the floor function which returns the largest integer no more than a . \square

Although the above solution is optimal, the structure of the sum-constellation as a function of λ is not straightforward enough. In the following part, we will give an asymptotically optimal solution to draw some useful insights and also reveal the merits of the proposed NOMA scheme.

C. Asymptotically Optimal Solution when the Transmission Rates of Both Users Are High

For the considered two-user system, the most interesting case is when the transmission rates of both users go to infinity [54], [58]. In a such case, we have $\lim_{M_1 \rightarrow \infty} \frac{M_1^2 - 1}{M_1^2} = 1$ and

$\lim_{M_2 \rightarrow \infty} \frac{M_2^2 - 1}{M_2^2} = 1$ and then $\beta(M_1)$ in (15) will converge to $\tilde{\beta}(\tilde{M}_1)$, such that:

$$\tilde{\beta}(\tilde{M}_1) = \begin{cases} \frac{M^2}{\lambda \tilde{M}_1^2}, & \text{if } 1 \leq \tilde{M}_1 \leq \frac{1}{\sqrt{\lambda}}; \\ M^2, & \text{if } 1 \leq \frac{1}{\sqrt{\lambda}} < \tilde{M}_1 \leq M; \\ \frac{M^2}{\lambda}, & \text{if } \frac{1}{M} \leq \frac{\tilde{M}_1}{M} \leq \frac{1}{\sqrt{\lambda}} < 1; \\ \tilde{M}_1^2, & \text{if } \frac{1}{\sqrt{\lambda}} < \frac{\tilde{M}_1}{M} \leq 1. \end{cases} \quad (16)$$

Problem 4 (*Asymptotically optimal rate-allocation problem in MAC under a sum-rate constraint*): We intend to solve the following optimization problem by adjusting \tilde{M}_1 and \tilde{M}_2 subject to a sum-rate constraint, given by:

$$\min_{\tilde{M}_1, \tilde{M}_2} \tilde{\beta}(\tilde{M}_1) \quad \text{s.t.} \quad \log_2 \tilde{M}_1 + \log_2 \tilde{M}_2 = \log_2 M, \quad (17)$$

where $\tilde{\beta}(\tilde{M}_1)$ is defined in (16), and \tilde{M}_1, \tilde{M}_2 are powers of 2. ■

Since the objective function is a simple piecewise function of \tilde{M}_1 , we are ready to formally give our solutions with no need of proof:

Theorem 3: Asymptotically optimal solution: The asymptotically optimal solution to Problem 4 is given by:

- 1) If $\lambda \leq 1$, we have $\tilde{M}_1^* = \min \{2^{\lfloor \log_2 \frac{1}{\sqrt{\lambda}} \rfloor + 1}, M\}$ and $\tilde{M}_2^* = \frac{M}{\tilde{M}_1^*}$;
- 2) If $\lambda > 1$, we have $\tilde{M}_1^* = \max \{2^{\lfloor \log_2 \frac{M}{\sqrt{\lambda}} \rfloor}, 1\}$ and $M_2^* = \frac{M}{\tilde{M}_1^*}$. ■

We have the following remark on the asymptotically optimal solution:

Remark 3: We consider the case in a high SNR regime and with near-far effect such that $\frac{1}{2} \log(1 + \frac{P_1|h_1|^2}{2\sigma^2}) \gg \frac{1}{2} \log(1 + \frac{P_2|h_2|^2}{2\sigma^2}) \gg 1$. We then have the following two cases:

- **Case 1:** The sum-rate is relatively low such that $M^2 \leq \frac{1}{\lambda}$: In this case, with Theorem 3, we have $\tilde{M}_1^* = \min \{2^{\lfloor \log_2 \frac{1}{\sqrt{\lambda}} \rfloor + 1}, M\} = M$ and $\tilde{M}_2^* = M/\tilde{M}_1^* = 1$. In other words, the channel should be solely allocated to the user with stronger channel, and our scheme degrades into the OMA method with the resulting minimum Euclidean distance $d_{\text{noma}} = \sqrt{\frac{3P_1}{2M^2}}|h_1|$.
- **Case 2:** The sum-rate is high enough such that $M^2 > \frac{1}{\lambda}$: Likewise, by Theorem 3, we have $\tilde{M}_1^* = \min \{2^{\lfloor \log_2 \frac{1}{\sqrt{\lambda}} \rfloor + 1}, M\} = 2^{\lfloor \log_2 \frac{1}{\sqrt{\lambda}} \rfloor + 1} \approx \frac{1}{\sqrt{\lambda}} = \frac{\sqrt{P_1}|h_1|}{\sqrt{P_2}|h_2|}$ and $\tilde{M}_2^* = M/\tilde{M}_1^* \approx \frac{\sqrt{P_2}|h_2|}{\sqrt{P_1}|h_1|}M$. Now, by (12), we can attain $d_{\text{noma}} = \sqrt{\frac{3P_1}{2\tilde{M}_2^{*2}(\tilde{M}_1^{*2}-1)}}|h_1| \approx \sqrt{\frac{3P_1}{2M^2}}|h_1|$.

Overall, for the proposed NOMA design in a high SNR regime and with near-far effect, if the sum-rate is low, the weak user should keep silent and the channel resources are solely allocated to the user with a stronger channel. On the other hand, if the sum-rate is high enough, the minimum

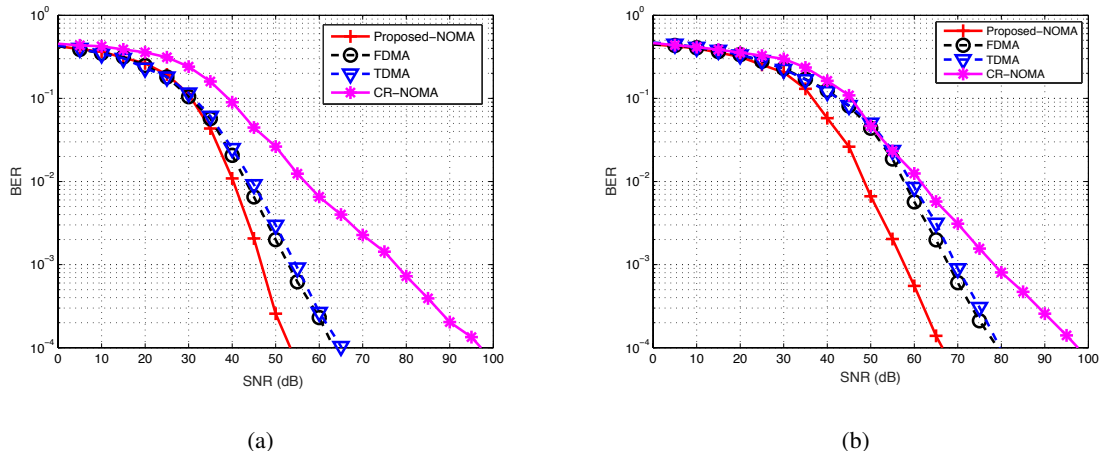


Fig. 1. Comparison between the Proposed-NOMA, CR-NOMA, TDMA and FDMA methods where 64-QAM is used for our case and 64-PSK is used for CR-based method: (a) $(\delta_1^2, \delta_2^2) = (1, 1)$, (b) $(\delta_1^2, \delta_2^2) = (1, 1/64)$.

Euclidean distance of the proposed NOMA design is close to that when only the strong user transmits free of interference. This means that in our scheme, the support of the weak user to transmit at a non-zero rate together with the strong user will cause almost no degradation to the system performance. But, the rate of the weak user highly depends on the near-far effect.

V. SIMULATION RESULTS AND DISCUSSIONS

In this section, we carry out computer simulations to verify the effectiveness of our NOMA design relative to the CR-NOMA design proposed in [40] and the OMA methods including TDMA and frequency-division multiple access (FDMA) schemes in various channel conditions and system configurations. More specifically, we consider both cases where the transmission rates are fixed or adaptive to channel states. Without loss of generality, we assume that $P_1 = P_2 = 1$ and the system signal-to-noise ratio (SNR) is defined by $\rho \triangleq 1/2\sigma^2$. All channels are subject to Rayleigh fading such that $h_k \sim \mathcal{CN}(0, 2\delta_k^2)$, $k = 1, 2$.

A. Comparison of Average Error Performance with Fixed Transmission Rate

We first consider the case where the transmission rates of both users are predetermined, i.e., the constellation sizes M_1^2 and M_2^2 are fixed. For convenience, we assume that both users transmit alternatively by using half of the total time slots or half of the available frequency band in TDMA and FDMA, respectively. In both methods, to maintain the same data rate for each user, we should increase the constellation sizes by using M_1^4 - and M_2^4 -ary QAM constellations

instead. There is no interference occurring at the receiver side since the channels are orthogonal to each other. It is worth mentioning that, for both TDMA and FDMA, we assume that the instantaneous transmit power of each user remains the same as in the NOMA. For FDMA method, as the total bandwidth of each user is halved, the equivalent noise at the receiver side also reduces by half compared with the TDMA method. Therefore, we would expect the FDMA scheme has an around 3dB SNR gain compared with TDMA method. For the CR-NOMA, we let each user transmit at the maximum allowable power by using constellations $\left\{ \exp\left(\frac{j2\pi k}{N}\right) \right\}_{k=0}^{N-1}$ and $\left\{ \exp\left(\frac{j2\pi k + j\pi}{N}\right) \right\}_{k=0}^{N-1}$ as proposed in [40] for users S_1 and S_2 , respectively.

We first compare the average BER of all the schemes where the variances of the channel coefficients are the same, i.e., $(\delta_1^2, \delta_2^2) = (1, 1)$ in Fig. 1(a). In the simulation, without loss of generality, we assume that each user adopts 64-QAM for the proposed NOMA design and 64-PSK is used by each user in CR-NOMA. Meanwhile, for TDMA and FDMA methods, each user uses 4096-QAM. As can be observed from Fig. 1(a) that, the proposed NOMA design outperforms all the designs in moderate and high SNR regimes. In addition, the FDMA method has a better error performance than the TDMA scheme as expected. The CR-NOMA has the highest BER due to the fact that the PSK constellation has a smaller Euclidean distance under the same power constraint compared with QAM constellation.

In the following simulation, we take the near-far effect into consideration by letting $(\delta_1^2, \delta_2^2) = (1, 1/64)$ as shown in Fig. 1(b). Likewise, the proposed NOMA design has the lowest BER compared with all the benchmark schemes. Also, we can observe that the gap between the proposed NOMA and the FDMA as well as TDMA is larger than that in the case of equal channel gain. For example, at the BER 10^{-3} , the proposed NOMA has around 5dB SNR gain in Fig. 1(a), while the SNR gain is approximately 10dB in Fig. 1(b). Interestingly, we also observe that the error performance of CR-NOMA improves substantially compared to TDMA and FDMA in this case with near-far effect.

From both Figs. 1(a) and 1(b), we can observe that the performance gain of NOMA is highly related to the relative strength of the channel coefficients. To show this phenomenon clearly, we now study the BER against the relative strength of the channel coefficients under different SNRs. More specifically, in Fig. 2(a), we set the variance of user S_1 as $\delta_1^2 = 1$, and we plot the BER against the variance of user S_2 , i.e., δ_2^2 , in dB. It can be observed from Fig. 2(a) that, for $\rho = 40$ dB (i.e., the SNR is relatively low relative to the target transmission rate), our proposed NOMA scheme outperforms all the benchmark schemes. When δ_2^2 is less than 1 (i.e., less than

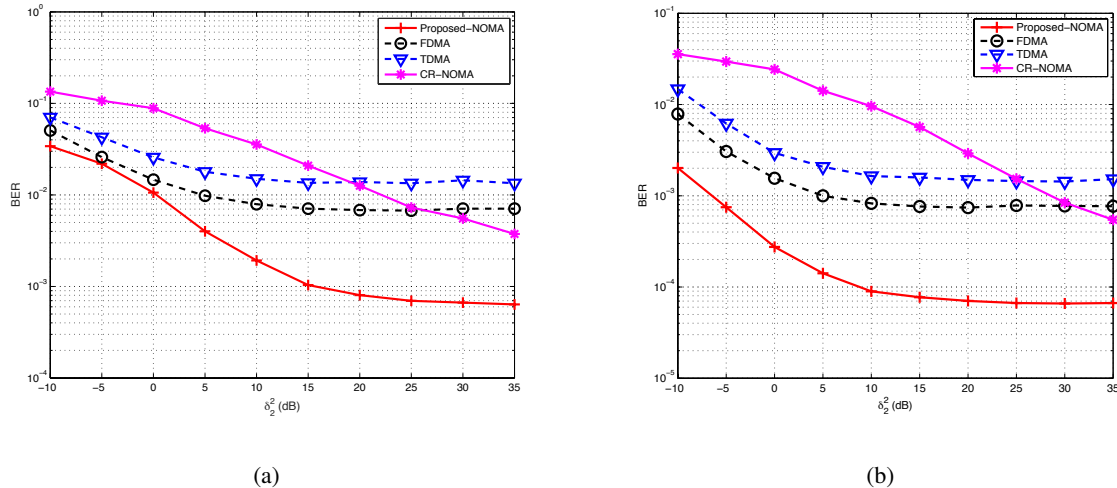


Fig. 2. Comparison between the Proposed-NOMA with CR-NOMA, TDMA, and FDMA methods, 64-QAM are used for our case and 64-PSK are used for CR based method with (a) $\rho = 40\text{dB}$. (b) $\rho = 50\text{dB}$.

0dB), the error performance is mainly limited by user S_1 and even if δ_2^2 equals to 1, the BER gain of the proposed NOMA method is still marginal. However, with the increase of δ_2^2 , the BER gain of the proposed NOMA method increases and finally gets saturated. Actually, when δ_2^2 is extremely large, the BER of the proposed NOMA is close to the system with one user transmitting with 64-QAM in both orthogonal blocks, while for the OMA method, it saturates as one user transmits using 4096-QAM in one block. This validates our observation that the proposed NOMA has a higher SNR gain when there is near-far effect. With the increase of δ_2^2 , the performance of CR-NOMA improves dramatically and it eventually outperforms the OMA methods. However, the BER performance is poor when the channel gains of the two users are close. This is due to the fact that with the same spectral efficiency, a PSK constellation has a smaller minimum Euclidean distance than a QAM constellation. Moreover, the sum-constellation of two PSK constellations at the receiver does not have a good geometric structure. In Fig. 2(b), we can see that with the near-far effect, the BER gain of the proposed NOMA also become more significant. The BER gain of the proposed NOMA is evident even if $\delta_2^2 = 1$, which coincides well with the phenomenon observed in Fig. 1.

B. Comparison of Average Error Performance with Optimal Rate Allocation

We now compare the average error performance of our proposed NOMA using the optimal rate allocation (see Sec. IV) with that of all the benchmark schemes. Note that for TDMA and FDMA,

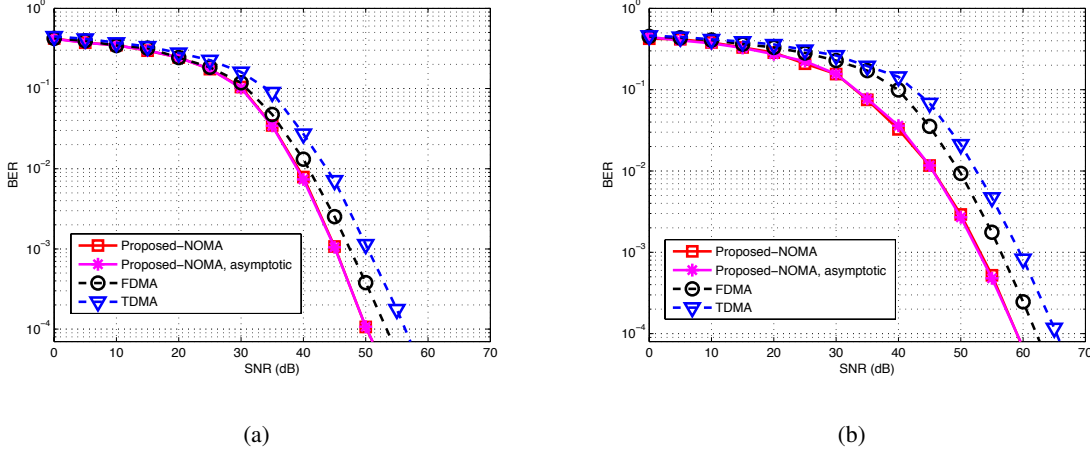


Fig. 3. Comparison between proposed-NOMA, TDD and FDD methods, 64-QAM are used with $M = 64$. (a) $(\delta_1^2, \delta_2^2) = (1, 1)$, (b) $(\delta_1^2, \delta_2^2) = (1, 1/64)$.

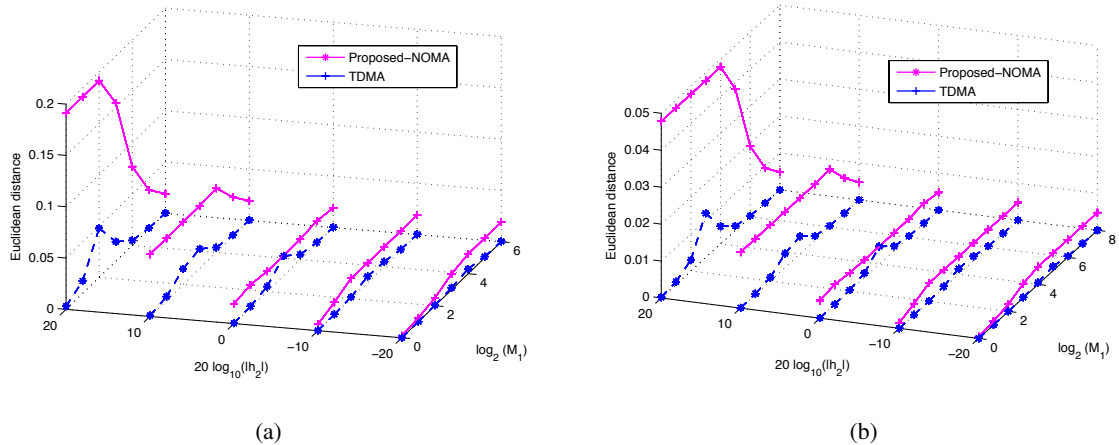


Fig. 4. Comparison of the minimum Euclidean distance of the proposed-NOMA (i.e., d_{noma} given in (12)) and that of TDMA method (d_{oma} given in (13)) with $|h_1| = 1$ for different $|h_2|$ and M_1 (a) $M = 64$, (b) $M = 256$.

we should find the optimal values of M_1 and M_2 satisfying $M = M_1 M_2$, to maximize d_{oma} given in (13). Without loss of generality, we set $M = 64$ and we consider both cases without and with near-far effect as plotted in Figs 3(a) and 3(b), respectively. As shown and explained in [27], the superiority of NOMA over OMA can be reduced when both of them adopt the optimal resource allocation. Here, we make similar observations by comparing Fig. 3 with Fig. 1. Nevertheless, as showed in Fig. 3, NOMA yields a considerable performance gain compared to OMA even they both employ the optimal resource allocation, and this gain can further be enlarged by the near-far effect. For example, at the BER of 10^{-3} , the proposed NOMA has about 3dB SNR gain

without near-far effect, which increases to 5dB with near-far effect. Moreover, we observe that the performance achieved by the asymptotically optimal rate allocation tightly approaches that of the optimal rate allocation solution, which validates our analysis in Sec. IV-C.

C. Comparison of the Minimum Euclidean Distance

At last, we compare the minimum Euclidean distance of the proposed NOMA design with that of TDMA method in Fig. 4. It can be observed that our proposed NOMA design achieves larger minimum Euclidean distance than TDMA method in all simulated cases, which validates the result presented in Corollary 2. We can also see that the stronger the near-far effect is, the larger the performance gap between the proposed NOMA and TDMA. More importantly, for the proposed NOMA, when we enlarge M_1 , there is a large interval in which the minimum Euclidean distance of NOMA (i.e., d_{noma}) will remain almost unchanged, while that of TDMA only has one peak among the considered range of M_1 . This indicates that the proposed NOMA has a larger degree of freedom in adaptive rate allocation than that of TDMA under the condition of causing nearly no degradation of system error performance.

VI. CONCLUSIONS

In this paper, we have presented a practical design framework for the non-orthogonal multiple access (NOMA) scheme in a classical two-user multiple access channel (MAC) with quadrature amplitude modulation (QAM) constellations at both users, the sizes of which are not necessarily the same. More specifically, we aimed to maximize the minimum Euclidean distance of the sum-constellation at the receiver by adjusting the instantaneous transmit power and phase of each user under an individual average power constraint. The design objective was formulated into a *mixed continuous-discrete* optimization problem. By introducing a new mathematical concept termed *punched Farey sequence* and investigating its fundamental properties, we managed to attain a compact closed-form solution. Based on the obtained solution, an adaptive rate allocation was performed to further maximize the minimum Euclidean distance of the received sum-constellation under a sum-rate constraint; a high-rate asymptotic approximation solution was also proposed to extract more insights on the NOMA design. Computer simulations were conducted to verify our derivation under various channel configurations, and the simulation results demonstrated that our proposed NOMA scheme outperforms OMA and existing NOMA significantly and the performance gap can be further enlarged when there is a near-far effect between the users.

APPENDIX

A. Proof of Property 1

1) We first prove that $\frac{n_1}{m_1} < \frac{n_1+n_2}{m_1+m_2}$, which can be showed by calculating $\frac{n_1+n_2}{m_1+m_2} - \frac{n_1}{m_1} = \frac{m_1n_2 - m_2n_1}{m_1(m_1+m_2)} > 0$, since $\frac{n_1}{m_1} < \frac{n_2}{m_2}$. The rest cases can be proved in a similar fashion and hence are omitted.

2) We now prove that $m_1n_2 - m_2n_1 = 1$ and it also gives the construction of the term which succeeds $\frac{n_1}{m_1}$ in \mathfrak{P}_K^L . First of all, since $\langle m_1, n_1 \rangle = 1$, the following equation

$$m_1n - mn_1 = 1 \quad (18)$$

has integer solutions in m, n such that $m = m_0 + rm_1, n = n_0 + rn_1$ for any integer r , where m_0, n_0 is a particular set of solutions to (18) and $\langle m, n \rangle = 1$ [50, Thm. 25]. As $\frac{n_1}{m_1} \in \mathfrak{P}_K^L$, we have $0 \leq n_1 \leq L$ and $0 \leq m_1 \leq K$. Then, we can choose m, n satisfying either condition:

$$\text{Case 1 : } K - m_1 < m \leq K, \text{ and } 0 < n \leq L; \quad (19a)$$

$$\text{Case 2 : } 0 < m \leq K - m_1, \text{ and } L - n_1 < n \leq L. \quad (19b)$$

Now, since $\frac{n}{m}$ is in its lowest terms (i.e., $\langle m, n \rangle = 1$), and for either case we have $0 < m \leq K$, $0 < n \leq L$, we conclude that $\frac{n}{m}$ is a fraction of \mathfrak{P}_K^L . In what follows, we will show that either Case 1 or 2 will generate the next term which comes after $\frac{n_1}{m_1}$ in \mathfrak{P}_K^L .

Case 1: From (18), $\frac{n}{m} = \frac{n_1}{m_1} + \frac{1}{m_1m} > \frac{n_1}{m_1}$, hence $\frac{n}{m}$ comes after $\frac{n_1}{m_1}$ in \mathfrak{P}_K^L . Then, if $\frac{n}{m}$ is not $\frac{n_2}{m_2}$, it will come after $\frac{n_2}{m_2}$, and then

$$\frac{n_2}{m_2} - \frac{n_1}{m_1} = \frac{m_1n_2 - m_2n_1}{m_1m_2} \geq \frac{1}{m_1m_2}; \quad \frac{n}{m} - \frac{n_2}{m_2} = \frac{m_2n - mn_2}{m_2m} \geq \frac{1}{m_2m}. \quad (20)$$

As a result, by jointly considering (18) and (20), we have $\frac{1}{m_1m} \stackrel{(a)}{=} \frac{m_1n - mn_1}{m_1m} = \frac{n}{m} - \frac{n_1}{m_1} = \frac{n}{m} - \frac{n_2}{m_2} + \frac{n_2}{m_2} - \frac{n_1}{m_1} \stackrel{(b)}{\geq} \frac{1}{m_2m} + \frac{1}{m_1m_2} = \frac{m_1+m}{m_1m_2m} \stackrel{(c)}{>} \frac{K}{m_1m_2m} \stackrel{(d)}{\geq} \frac{1}{m_1m}$, where (a) follows from (18); inequality (b) holds since (20); inequality (c) follows from (19a) and (d) is true since $\frac{n_2}{m_2} \in \mathfrak{P}_K^L$.

This is a contradiction, and therefore $\frac{n}{m}$ must be $\frac{n_2}{m_2}$, and hence $m_1n_2 - m_2n_1 = 1$.

Case 2: As in Case 1, according to (18), $\frac{n}{m} = \frac{n_1}{m_1} + \frac{1}{m_1m} > \frac{n_1}{m_1}$, and hence $\frac{n}{m}$ comes after $\frac{n_1}{m_1}$ in \mathfrak{P}_K^L . As a result, if $\frac{n}{m}$ is not $\frac{n_2}{m_2}$, it comes after $\frac{n_2}{m_2}$, and we have

$$\frac{m_1}{n_1} - \frac{m_2}{n_2} = \frac{m_1n_2 - m_2n_1}{n_1n_2} \geq \frac{1}{n_1n_2}; \quad \frac{m_2}{n_2} - \frac{m}{n} = \frac{m_2n - mn_2}{n_2n} \geq \frac{1}{n_2n}. \quad (21)$$

Likewise, we conclude that $\frac{1}{n_1n} \stackrel{(a)}{=} \frac{m_1n - mn_1}{n_1n} = \frac{m_1}{n_1} - \frac{m}{n} = \frac{m_1}{n_1} - \frac{m_2}{n_2} + \frac{m_2}{n_2} - \frac{m}{n} \stackrel{(b)}{\geq} \frac{1}{n_1n_2} + \frac{1}{n_2n} = \frac{n+n_1}{n_1n_2n} \stackrel{(c)}{>} \frac{L}{n_1n_2n} \stackrel{(d)}{\geq} \frac{1}{n_1n}$, where (a) follows from (18), inequality (b) holds as a result of (21), and

inequality (c) follows from (19b), and (d) is true since $\frac{n_2}{m_2} \in \mathfrak{P}_K^L$. There is also a contradiction, therefore $\frac{n}{m}$ must be $\frac{n_2}{m_2}$, and thus $m_1 n_2 - m_2 n_1 = 1$. 3) From the above proof, i.e., (19a) and (19b), we can observe that: (a) If $n_1 + n_2 \leq L$, then $m_1 + m_2 > K$; (b) If $m_1 + m_2 \leq K$, then $n_1 + n_2 > L$.

4) From (19a) and (19b), we can observe that, $m_1 + m_2 > 0$ (i.e., $m_1 + m_2 \geq 1$) and $n_1 + n_2 > 0$ (i.e., $n_1 + n_2 \geq 1$). First, we consider the case $\frac{n_1}{m_1} = \frac{0}{1}$. As $n_1 = 0$, then by solving (18) of Case 1 in the above discussion, we have $n_2 = 1$. By (19a), we attain $K - 1 < m_2 \leq K$, i.e., $m_2 = K$. Now, we attain two adjacent terms $\frac{n_1}{m_1} = \frac{0}{1}$ and $\frac{n_2}{m_2} = \frac{1}{K}$ such that $n_1 + n_2 = 1$ and $m_1 + m_2 = K + 1$. Similarly, we can find adjacent terms $\frac{n_1}{m_1} = \frac{L}{1}$ and $\frac{n_2}{m_2} = \frac{1}{0}$ such that $m_1 + m_2 = 1$ and $n_1 + n_2 = L + 1$.

This completes the proof of Property 1. \square

B. Proof of Property 2

By Property 1, we have $m_1 n_2 - m_2 n_1 = 1$, $m_2 n_3 - m_3 n_2 = 1$. Then, solving the following equations: $m_3 m_1 n_2 - m_3 m_2 n_1 = m_3$, $m_1 m_2 n_3 - m_1 m_3 n_2 = m_1$, $n_3 m_1 n_2 - n_3 m_2 n_1 = n_3$, $n_1 m_2 n_3 - n_1 m_3 n_2 = n_1$, for m_2, n_2 , we attain $m_2(m_1 n_3 - m_3 n_1) = m_1 + m_3$, $n_2(m_1 n_3 - m_3 n_1) = n_1 + n_3$. As $m_1 n_3 - m_3 n_1 \neq 0$, we have $\frac{n_2}{m_2} = \frac{n_1 + n_3}{m_1 + m_3}$. The property is proved. \square

C. Proof of Property 3

From the assumption, we have $\frac{n_2}{m_2} - \frac{n_1 + n_3}{m_1 + m_3} = \frac{m_1 n_2 + m_3 n_2 - m_2 n_1 - m_2 n_3}{m_2(m_1 + m_3)} = \frac{m_1 n_2 - m_2 n_1 - 1}{m_2(m_1 + m_2)} \geq 0$;
 $\frac{n_2 + n_4}{m_2 + m_4} - \frac{n_3}{m_3} = \frac{m_3 n_2 + m_3 n_4 - m_2 n_3 - m_4 n_3}{m_3(m_2 + m_4)} = \frac{m_3 n_4 - m_4 n_3 - 1}{m_3(m_2 + m_4)} \geq 0$. The completes the proof. \square

D. Proof of Proposition 2

Recall that $d(m, n) = \left| |\tilde{h}_1| \tilde{w}_1 n - |\tilde{h}_2| \tilde{w}_2 m \right|$. Therefore, for $\frac{|\tilde{h}_2| \tilde{w}_2}{|\tilde{h}_1| \tilde{w}_1} \in \left(\frac{n_1}{m_1}, \frac{n_2}{m_2} \right)$, we have $d(m_1, n_1) - d(m_2, n_2) = \left| |\tilde{h}_1| \tilde{w}_1 n_1 - |\tilde{h}_2| \tilde{w}_2 m_1 \right| - \left| |\tilde{h}_1| \tilde{w}_1 n_2 - |\tilde{h}_2| \tilde{w}_2 m_2 \right| = -|\tilde{h}_1| \tilde{w}_1 n_1 + |\tilde{h}_2| \tilde{w}_2 m_1 - |\tilde{h}_1| \tilde{w}_1 n_2 + |\tilde{h}_2| \tilde{w}_2 m_2 = (m_1 + m_2) |\tilde{h}_1| \tilde{w}_1 \left(\frac{|\tilde{h}_2| \tilde{w}_2}{|\tilde{h}_1| \tilde{w}_1} - \frac{n_1 + n_2}{m_1 + m_2} \right)$. The results in Proposition 2 can be readily obtained, and we complete the proof. \square

E. Proof of of Proposition 3

Proof: As $\frac{n_1}{m_1}$ and $\frac{n_4}{m_4}$ are arbitrarily chosen, Proposition 3 is equivalent to

- 1) If $\frac{|\tilde{h}_2| \tilde{w}_2}{|\tilde{h}_1| \tilde{w}_1} \in \left(\frac{n_2}{m_2}, \frac{n_2 + n_3}{m_2 + m_3} \right)$, then $d(m_2, n_2) < d(m_3, n_3)$, $d(m_2, n_2) < d(m_4, n_4)$, and $d(m_2, n_2) < d(m_1, n_1)$;

- 2) If $\frac{|\tilde{h}_2|\tilde{w}_2}{|\tilde{h}_1|\tilde{w}_1} \in \left(\frac{n_2+n_3}{m_2+m_3}, \frac{n_3}{m_3}\right)$, then $d(m_3, n_3) < d(m_2, n_2)$, $d(m_3, n_3) < d(m_1, n_1)$, and $d(m_3, n_3) < d(m_4, n_4)$.

First, by Proposition 2, we have

- 1) If $\frac{|\tilde{h}_2|\tilde{w}_2}{|\tilde{h}_1|\tilde{w}_1} \in \left(\frac{n_2}{m_2}, \frac{n_2+n_3}{m_2+m_3}\right)$, then $d(m_2, n_2) < d(m_3, n_3)$ and $d(m_2, n_2) < d(m_4, n_4)$;
 2) If $\frac{|\tilde{h}_2|\tilde{w}_2}{|\tilde{h}_1|\tilde{w}_1} \in \left(\frac{n_2+n_3}{m_2+m_3}, \frac{n_3}{m_3}\right)$, then $d(m_3, n_3) < d(m_1, n_1)$ and $d(m_3, n_3) < d(m_2, n_2)$.

Then, we want to show that:

- 1) If $\frac{|\tilde{h}_2|\tilde{w}_2}{|\tilde{h}_1|\tilde{w}_1} \in \left(\frac{n_2}{m_2}, \frac{n_2+n_3}{m_2+m_3}\right)$, then $d(m_2, n_2) < d(m_1, n_1)$;
 2) If $\frac{|\tilde{h}_2|\tilde{w}_2}{|\tilde{h}_1|\tilde{w}_1} \in \left(\frac{n_2+n_3}{m_2+m_3}, \frac{n_3}{m_3}\right)$, then $d(m_3, n_3) < d(m_4, n_4)$.

The first case can be proved by considering $d(m_1, n_1) - d(m_2, n_2) = \left| |\tilde{h}_1|\tilde{w}_1 n_1 - |\tilde{h}_2|\tilde{w}_2 m_1 \right| - \left| |\tilde{h}_1|\tilde{w}_1 n_2 - |\tilde{h}_2|\tilde{w}_2 m_2 \right| = |\tilde{h}_1|\tilde{w}_1 \left(\frac{|\tilde{h}_2|\tilde{w}_2}{|\tilde{h}_1|\tilde{w}_1} (m_1 - m_2) - (n_1 - n_2) \right)$. As $\frac{|\tilde{h}_2|\tilde{w}_2}{|\tilde{h}_1|\tilde{w}_1} \in \left(\frac{n_2}{m_2}, \frac{n_2+n_3}{m_2+m_3}\right)$, then $d(m_1, n_1) - d(m_2, n_2) \geq 0$ is true if $\frac{n_2}{m_2}(m_1 - m_2) - (n_1 - n_2) \geq 0$ and $\frac{n_2+n_3}{m_2+m_3}(m_1 - m_2) - (n_1 - n_2) \geq 0$. We know that $\frac{n_2}{m_2}(m_1 - m_2) - (n_1 - n_2) = (m_1 n_2 - m_2 n_1)/m_2 > 0$, and $\frac{n_2+n_3}{m_2+m_3}(m_1 - m_2) - (n_1 - n_2) = ((n_2 + n_3)(m_1 - m_2) - (m_2 + m_3)(n_1 - n_2))/(m_2 + m_3) = ((m_1 + m_3)n_2 - m_2(n_1 + n_3) + m_1 n_3 - m_3 n_1)/(m_2 + m_3) > 0$, where the inequality is always true by Property 3.

Likewise, the second case can be proved by considering $d(m_4, n_4) - d(m_3, n_3) = \left| |\tilde{h}_1|\tilde{w}_1 n_4 - |\tilde{h}_2|\tilde{w}_2 m_4 \right| - \left| |\tilde{h}_1|\tilde{w}_1 n_3 - |\tilde{h}_2|\tilde{w}_2 m_3 \right| = |\tilde{h}_1|\tilde{w}_1 \left(\frac{|\tilde{h}_2|\tilde{w}_2}{|\tilde{h}_1|\tilde{w}_1} (m_3 - m_4) - (n_3 - n_4) \right)$. As $\frac{|\tilde{h}_2|\tilde{w}_2}{|\tilde{h}_1|\tilde{w}_1} \in \left(\frac{n_2+n_3}{m_2+m_3}, \frac{n_3}{m_3}\right)$, then $d(m_4, n_4) - d(m_3, n_3) \geq 0$ is true if $\frac{n_3}{m_3}(m_3 - m_4) - (n_3 - n_4) \geq 0$ and $\frac{n_2+n_3}{m_2+m_3}(m_3 - m_4) - (n_3 - n_4) \geq 0$. We know that $\frac{n_3}{m_3}(m_3 - m_4) - (n_3 - n_4) = (n_3(m_3 - m_4) - m_3(n_3 - n_4))/m_3 = (m_3 n_4 - m_4 n_3)/m_3 > 0$, and $\frac{n_2+n_3}{m_2+m_3}(m_3 - m_4) - (n_3 - n_4) = ((n_2 + n_3)(m_3 - m_4) - (m_2 + m_3)(n_3 - n_4))/(m_2 + m_3) = (m_3(n_2 + n_4) - n_3(m_2 + m_4) + m_2 n_4 - m_4 n_2)/(m_2 + m_3) > 0$, where the inequality is always true by Property 3. We complete the proof. \square

F. Proof of Lemma 1

According to proposition 3 and notice that $\left(\frac{b_k}{a_k}, \frac{b_{k+1}}{a_{k+1}}\right) = \left(\frac{b_k}{a_k}, \frac{b_k+b_{k+1}}{a_k+a_{k+1}}\right) \cup \left(\frac{b_k+b_{k+1}}{a_k+a_{k+1}}, \frac{b_{k+1}}{a_{k+1}}\right)$, problem in (10) can be further divided into the following two sub-problems, and the overall solution is the maximum value of the two problems:

Problem 5 (Sub-problem 1): The optimization problem is stated as follows:

$$g_1\left(\frac{b_k}{a_k}, \frac{b_{k+1}}{a_{k+1}}\right) = \max_{(\tilde{w}_1, \tilde{w}_2)} |\tilde{h}_2|\tilde{w}_2 a_k - |\tilde{h}_1|\tilde{w}_1 b_k \quad (22a)$$

$$\text{s.t. } \frac{b_k}{a_k} \leq \frac{|\tilde{h}_2|\tilde{w}_2}{|\tilde{h}_1|\tilde{w}_1} < \frac{b_k + b_{k+1}}{a_k + a_{k+1}}, \quad 0 < \tilde{w}_1 \leq 1, \quad 0 < \tilde{w}_2 \leq 1. \quad (22b)$$

■

Problem 6 (Sub-problem 2): We aim to solve the following optimization problem:

$$g_2\left(\frac{b_k}{a_k}, \frac{b_{k+1}}{a_{k+1}}\right) = \max_{(\tilde{w}_1, \tilde{w}_2)} |\tilde{h}_1|\tilde{w}_1 b_{k+1} - |\tilde{h}_2|\tilde{w}_2 a_{k+1} \quad (23a)$$

$$\text{s.t. } \frac{b_k + b_{k+1}}{a_k + a_{k+1}} \leq \frac{|\tilde{h}_2|\tilde{w}_2}{|\tilde{h}_1|\tilde{w}_1} \leq \frac{b_{k+1}}{a_{k+1}}, \quad 0 < \tilde{w}_1 \leq 1, \quad 0 < \tilde{w}_2 \leq 1. \quad (23b)$$

■

We know that (22) is equivalent to

$$g_1\left(\frac{b_k}{a_k}, \frac{b_{k+1}}{a_{k+1}}\right) = \max_{(w_1, w_2)} |\tilde{h}_2|w_2 a_k - |\tilde{h}_1|w_1 b_k \quad (24a)$$

$$\text{s.t. } \frac{|\tilde{h}_2|(a_k + a_{k+1})}{|\tilde{h}_1|(b_k + b_{k+1})} w_2 < w_1 \leq \frac{a_k |\tilde{h}_2|}{b_k |\tilde{h}_1|} w_2, \quad 0 < w_1 \leq 1, \quad 0 < w_2 \leq 1. \quad (24b)$$

We can find that the objective function is a linear decreasing function of w_1 . Then, we let $w_1 = \frac{|\tilde{h}_2|(a_k + a_{k+1})}{|\tilde{h}_1|(b_k + b_{k+1})} w_2$, and the objective function can be reformulated by $|\tilde{h}_2|w_2 a_k - |\tilde{h}_1|w_1 b_k = (a_k(b_k + b_{k+1}) - b_k(a_k + a_{k+1})) \frac{|\tilde{h}_2|w_2}{b_k + b_{k+1}} \stackrel{(a)}{=} \frac{|\tilde{h}_2|w_2}{b_k + b_{k+1}}$, where (a) follows from Property 1. Now, the constraints on w_2 are $0 < w_2 \leq 1$, $0 < w_2 \leq \frac{|\tilde{h}_1|(b_k + b_{k+1})}{|\tilde{h}_2|(a_k + a_{k+1})}$. Therefore, the solution to (22) can be given as follows:

$$g_1\left(\frac{b_k}{a_k}, \frac{b_{k+1}}{a_{k+1}}\right) = \begin{cases} \frac{|\tilde{h}_2|}{b_k + b_{k+1}}, & \text{with } (\tilde{w}_1, \tilde{w}_2) = \left(\frac{|\tilde{h}_2|(a_k + a_{k+1})}{|\tilde{h}_1|(b_k + b_{k+1})}, 1\right), & \text{if } \frac{|\tilde{h}_2|}{|\tilde{h}_1|} \leq \frac{b_k + b_{k+1}}{a_k + a_{k+1}}; \\ \frac{|\tilde{h}_1|}{a_k + a_{k+1}}, & \text{with } (\tilde{w}_1, \tilde{w}_2) = \left(1, \frac{|\tilde{h}_1|(b_k + b_{k+1})}{|\tilde{h}_2|(a_k + a_{k+1})}\right), & \text{if } \frac{|\tilde{h}_2|}{|\tilde{h}_1|} > \frac{b_k + b_{k+1}}{a_k + a_{k+1}}. \end{cases} \quad (25)$$

Likewise, we note that (23) is equivalent to

$$g_2\left(\frac{b_k}{a_k}, \frac{b_{k+1}}{a_{k+1}}\right) = \max_{(\tilde{w}_1, \tilde{w}_2)} |\tilde{h}_1|\tilde{w}_1 b_{k+1} - |\tilde{h}_2|\tilde{w}_2 a_{k+1} \quad (26a)$$

$$\text{s.t. } \frac{(b_k + b_{k+1})|\tilde{h}_1|}{(a_k + a_{k+1})|\tilde{h}_2|} \tilde{w}_1 \leq \tilde{w}_2 \leq \frac{b_{k+1}|\tilde{h}_1|}{a_{k+1}|\tilde{h}_2|} \tilde{w}_1, \quad 0 < \tilde{w}_1 \leq 1, \quad 0 < \tilde{w}_2 \leq 1. \quad (26b)$$

By letting $\tilde{w}_2 = \frac{(b_k + b_{k+1})|\tilde{h}_1|}{(a_k + a_{k+1})|\tilde{h}_2|} \tilde{w}_1$, the objective function can be reformulated by $|\tilde{h}_1|\tilde{w}_1 b_{k+1} - |\tilde{h}_2|\tilde{w}_2 a_{k+1} = (b_{k+1}(a_k + a_{k+1}) - a_{k+1}(b_k + b_{k+1})) \frac{|\tilde{h}_1|\tilde{w}_1}{a_k + a_{k+1}} = \frac{|\tilde{h}_1|\tilde{w}_1}{a_k + a_{k+1}}$. The constraints on \tilde{w}_1 are $0 < \tilde{w}_1 \leq 1$ and $0 < \tilde{w}_1 < \frac{(a_k + a_{k+1})|\tilde{h}_2|}{(b_k + b_{k+1})|\tilde{h}_1|}$. Thus, we have

$$g_2\left(\frac{b_k}{a_k}, \frac{b_{k+1}}{a_{k+1}}\right) = \begin{cases} \frac{|\tilde{h}_2|}{b_k + b_{k+1}}, & \text{with } (\tilde{w}_1, \tilde{w}_2) = \left(\frac{|\tilde{h}_2|(a_k + a_{k+1})}{|\tilde{h}_1|(b_k + b_{k+1})}, 1\right), & \text{if } \frac{|\tilde{h}_2|}{|\tilde{h}_1|} \leq \frac{b_k + b_{k+1}}{a_k + a_{k+1}}; \\ \frac{|\tilde{h}_1|}{a_k + a_{k+1}}, & \text{with } (\tilde{w}_1, \tilde{w}_2) = \left(1, \frac{|\tilde{h}_1|(b_k + b_{k+1})}{|\tilde{h}_2|(a_k + a_{k+1})}\right), & \text{if } \frac{|\tilde{h}_2|}{|\tilde{h}_1|} > \frac{b_k + b_{k+1}}{a_k + a_{k+1}}. \end{cases} \quad (27)$$

Combining the two cases, we have the result in Lemma 1, and we complete the proof. \square

G. Proof of Theorem 1

Consider the punched Farey sequence $\mathfrak{F}_{M_2-1}^{M_1-1} = \left(\frac{b_1}{a_1}, \frac{b_2}{a_2}, \dots, \frac{b_C}{a_C}\right)$, where $C = |\mathfrak{F}_{M_2-1}^{M_1-1}|$. We consider each case separately as follows:

1) If $\frac{|\tilde{h}_2|}{|\tilde{h}_1|} \leq \frac{1}{M_2}$, we have $\frac{|\tilde{h}_2|}{|\tilde{h}_1|} \leq \frac{1}{M_2} = \frac{b_1+b_2}{a_1+a_2} \leq \frac{b_k+b_{k+1}}{a_k+a_{k+1}}, k = 1, \dots, C-1$. By Lemma 1, for each Farey interval, we can attain that $g\left(\frac{b_k}{a_k}, \frac{b_{k+1}}{a_{k+1}}\right) = \frac{|\tilde{h}_2|}{b_k+b_{k+1}}$, for $k = 1, \dots, C-1$. As a consequence, the minimum Euclidean distance d^* can be attained by taking the maximum value of the objective function over all the possible intervals, given by: $d^* = \max\left\{\frac{|\tilde{h}_2|}{b_1+b_2}, \dots, \frac{|\tilde{h}_2|}{b_{C-1}+b_C}\right\} = \frac{|\tilde{h}_2|}{b_1+b_2} = |\tilde{h}_2|$, where the optimality is attained when $(\tilde{w}_1^*, \tilde{w}_2^*) = (M_2 \frac{|\tilde{h}_2|}{|\tilde{h}_1|}, 1)$ with the help of Property 1, and hence $\frac{|\tilde{h}_1| \tilde{w}_1^*}{|\tilde{h}_2| \tilde{w}_2^*} = M_2$.

2) If $\frac{1}{M_2} < \frac{|\tilde{h}_2|}{|\tilde{h}_1|} \leq \frac{M_1}{M_2}$, we can suppose that $\frac{b_{\ell_1}+b_{\ell_1+1}}{a_{\ell_1}+a_{\ell_1+1}} < \frac{|\tilde{h}_2|}{|\tilde{h}_1|} \leq \frac{b_{\ell_1+1}+b_{\ell_1+2}}{a_{\ell_1+1}+a_{\ell_1+2}}$, where ℓ_1 can be determined upon the knowledge of $\frac{|\tilde{h}_2|}{|\tilde{h}_1|}$. Then, with the help of Lemma 1, we have

$$g\left(\frac{b_k}{a_k}, \frac{b_{k+1}}{a_{k+1}}\right) = \begin{cases} \frac{|\tilde{h}_1|}{a_k+a_{k+1}}, & k = 1, \dots, \ell_1; \\ \frac{|\tilde{h}_2|}{b_k+b_{k+1}}, & k = \ell_1 + 1, \dots, C-1. \end{cases}$$

First, for $a_k + a_{k+1}, k = 1, \dots, \ell_1$, we have the following two cases: (a) If $a_k + a_{k+1} \geq M_2$, then we have $\frac{1}{a_k+a_{k+1}} \leq \frac{1}{M_2}$; (b) If $a_k + a_{k+1} < M_2$ (i.e., $a_k + a_{k+1} \leq M_2 - 1$), then by Property 1, we have $b_k + b_{k+1} \geq M_1$ (i.e., $b_k + b_{k+1} > M_1 - 1$). From the assumption, we have $\frac{b_k+b_{k+1}}{a_k+a_{k+1}} \leq \frac{b_{\ell_1}+b_{\ell_1+1}}{a_{\ell_1}+a_{\ell_1+1}} < \frac{|\tilde{h}_2|}{|\tilde{h}_1|} \leq \frac{M_1}{M_2}$. Therefore, we have $\frac{1}{a_k+a_{k+1}} \leq \frac{M_1}{M_2(b_k+b_{k+1})} \leq \frac{1}{M_2}$. Combining the above two cases, we have

$$\frac{1}{a_k + a_{k+1}} \leq \frac{1}{M_2}, \quad k = 1, \dots, \ell_1. \quad (28)$$

Next, consider $b_k + b_{k+1}, k = \ell_1 + 1, \dots, C-1$ and we can show that: (a) If $b_k + b_{k+1} < M_1$ (i.e., $b_k + b_{k+1} \leq M_1 - 1$), then by Property 1, we have $a_k + a_{k+1} \geq M_2$ (i.e., $a_k + a_{k+1} > M_2 - 1$). As a consequence, we have $\frac{|\tilde{h}_2|}{|\tilde{h}_1|} \leq \frac{b_{\ell_1+1}+b_{\ell_1+2}}{a_{\ell_1+1}+a_{\ell_1+2}} \leq \frac{b_k+b_{k+1}}{a_k+a_{k+1}} \leq \frac{b_k+b_{k+1}}{M_2}$; (b) If $b_k + b_{k+1} \geq M_1$, then we have $\frac{|\tilde{h}_2|}{|\tilde{h}_1|} \leq \frac{M_1}{M_2} \leq \frac{b_k+b_{k+1}}{M_2}$. Combining both cases, we have

$$\frac{|\tilde{h}_1|}{M_2} \geq \frac{|\tilde{h}_2|}{b_k + b_{k+1}}, \quad k = \ell_1 + 1, \dots, C-1. \quad (29)$$

Now, with the help of (28) and (29), the overall minimum Euclidean distance is given by $d^* = \max\left\{\frac{|\tilde{h}_1|}{a_1+a_2}, \dots, \frac{|\tilde{h}_1|}{a_{\ell_1}+a_{\ell_1+1}}, \frac{|\tilde{h}_2|}{b_{\ell_1+1}+b_{\ell_1+2}}, \dots, \frac{|\tilde{h}_2|}{b_{C-1}+b_C}\right\} = \max\left\{\frac{|\tilde{h}_1|}{M_2}, \frac{|\tilde{h}_2|}{b_{\ell_1+1}+b_{\ell_1+2}}, \dots, \frac{|\tilde{h}_2|}{b_{C-1}+b_C}\right\} =$

$\frac{|\tilde{h}_1|}{M_2}$, where the optimality is attained when $(\tilde{w}_1^*, \tilde{w}_2^*) = (1, \frac{|\tilde{h}_1|}{M_2|\tilde{h}_2|})$ and as a result we have $\frac{|\tilde{h}_1|\tilde{w}_1^*}{|\tilde{h}_2|\tilde{w}_2^*} = M_2$.

3) If $\frac{M_1}{M_2} < \frac{|\tilde{h}_2|}{|\tilde{h}_1|} \leq M_1$, we can suppose that $\frac{b_{\ell_2}+b_{\ell_2+1}}{a_{\ell_2}+a_{\ell_2+1}} \leq \frac{|\tilde{h}_2|}{|\tilde{h}_1|} < \frac{b_{\ell_2+1}+b_{\ell_2+2}}{a_{\ell_2+1}+a_{\ell_2+2}}$. With the help of Lemma 1, we have

$$g\left(\frac{b_k}{a_k}, \frac{b_{k+1}}{a_{k+1}}\right) = \begin{cases} \frac{|\tilde{h}_1|}{a_k+a_{k+1}}, & k = 1, \dots, \ell_2; \\ \frac{|\tilde{h}_2|}{b_k+b_{k+1}}, & k = \ell_2 + 1, \dots, C - 1. \end{cases}$$

We first show that, for $b_k + b_{k+1}, k = \ell_2 + 1, \dots, C - 1$, (a) If $b_k + b_{k+1} \geq M_1$, then we have $\frac{1}{b_k+b_{k+1}} \leq \frac{1}{M_1}$; (b) If $b_k + b_{k+1} < M_1$, then by Property 1, we have $a_k + a_{k+1} \geq M_2$. From the assumption, we have $\frac{b_k+b_{k+1}}{a_k+a_{k+1}} \geq \frac{b_{\ell_2+1}+b_{\ell_2+2}}{a_{\ell_2+1}+a_{\ell_2+2}} > \frac{|\tilde{h}_2|}{|\tilde{h}_1|} > \frac{M_1}{M_2}$. Therefore, we have $\frac{1}{b_k+b_{k+1}} < \frac{M_2}{M_1(a_k+a_{k+1})} \leq \frac{1}{M_1}$. By jointly considering both cases, we have

$$\frac{1}{b_k + b_{k+1}} \leq \frac{1}{M_1}, \text{ for } k = \ell_2 + 1, \dots, C - 1. \quad (30)$$

Next, we consider $a_k + a_{k+1}, k = 1, \dots, \ell_2$, (a) If $a_k + a_{k+1} < M_2$, then by Property 1, we have $b_k + b_{k+1} \geq M_1$; As a result, $\frac{M_1}{a_k+a_{k+1}} \leq \frac{b_k+b_{k+1}}{a_k+a_{k+1}} \leq \frac{b_{\ell_2}+b_{\ell_2+1}}{a_{\ell_2}+a_{\ell_2+1}} \leq \frac{|\tilde{h}_2|}{|\tilde{h}_1|}$. (b) If $a_k + a_{k+1} \geq M_2$, then $\frac{M_1}{a_k+a_{k+1}} \leq \frac{M_1}{M_2} < \frac{|\tilde{h}_2|}{|\tilde{h}_1|}$. Combining both cases, we conclude that

$$\frac{|\tilde{h}_1|}{a_k + a_{k+1}} \leq \frac{|\tilde{h}_2|}{M_1}, k = 1, \dots, \ell_2. \quad (31)$$

Therefore, with the help of (30) and (31), the overall minimum Euclidean distance is $d^* = \max \left\{ \frac{|\tilde{h}_1|}{a_1+a_2}, \dots, \frac{|\tilde{h}_1|}{a_{\ell_2}+a_{\ell_2+1}}, \frac{|\tilde{h}_2|}{b_{\ell_2+1}+b_{\ell_2+2}}, \dots, \frac{|\tilde{h}_2|}{b_{C-1}+b_C} \right\} = \max \left\{ \frac{|\tilde{h}_1|}{a_1+a_2}, \dots, \frac{|\tilde{h}_1|}{a_{\ell_2}+a_{\ell_2+1}}, \frac{|\tilde{h}_2|}{M_1} \right\} = \frac{|\tilde{h}_2|}{M_1}$, where the optimality is attained when $(\tilde{w}_1^*, \tilde{w}_2^*) = \left(\frac{|\tilde{h}_2|}{M_1|\tilde{h}_1|}, 1 \right)$ and as a result, $d^* = \frac{|\tilde{h}_2|}{M_1}$ and $\frac{|\tilde{h}_1|\tilde{w}_1^*}{|\tilde{h}_2|\tilde{w}_2^*} = \frac{1}{M_1}$.

4) If $M_1 < \frac{|\tilde{h}_2|}{|\tilde{h}_1|}$, then $\frac{b_k+b_{k+1}}{a_k+a_{k+1}} \leq M_1 < \frac{|\tilde{h}_2|}{|\tilde{h}_1|}$, for $k = 1, \dots, C - 1$. By using Lemma 1, $g\left(\frac{b_k}{a_k}, \frac{b_{k+1}}{a_{k+1}}\right) = \frac{|\tilde{h}_1|}{a_k+a_{k+1}}$ for $k = 1, \dots, C - 1$, and $d^* = \max \left\{ \frac{|\tilde{h}_1|}{a_1+a_2}, \dots, \frac{|\tilde{h}_1|}{a_{C-1}+a_C} \right\} = \frac{|\tilde{h}_1|}{a_{C-1}+a_C} = |\tilde{h}_1|$, where the optimality is attained when $(\tilde{w}_1, \tilde{w}_2) = (1, M_1 \frac{|\tilde{h}_1|}{|\tilde{h}_2|})$ with the help of Property 1, and as a result, $\frac{|\tilde{h}_1|\tilde{w}_1^*}{|\tilde{h}_2|\tilde{w}_2^*} = \frac{1}{M_1}$.

The solution to Problem 1 can be summarized as

- If $\frac{|\tilde{h}_2|}{|\tilde{h}_1|} \leq \frac{1}{M_2}$, then $(\tilde{w}_1^*, \tilde{w}_2^*) = (M_2 \frac{|\tilde{h}_2|}{|\tilde{h}_1|}, 1)$, $d^* = |\tilde{h}_2|$, and $\frac{|\tilde{h}_1|\tilde{w}_1^*}{|\tilde{h}_2|\tilde{w}_2^*} = M_2$;
- If $\frac{1}{M_2} < \frac{|\tilde{h}_2|}{|\tilde{h}_1|} \leq \frac{M_1}{M_2}$, then $(\tilde{w}_1^*, \tilde{w}_2^*) = (1, \frac{|\tilde{h}_1|}{M_2|\tilde{h}_2|})$, $d^* = \frac{|\tilde{h}_1|}{M_2}$, and $\frac{|\tilde{h}_1|\tilde{w}_1^*}{|\tilde{h}_2|\tilde{w}_2^*} = M_2$;
- If $\frac{M_1}{M_2} < \frac{|\tilde{h}_2|}{|\tilde{h}_1|} \leq M_1$, then $(\tilde{w}_1^*, \tilde{w}_2^*) = (\frac{|\tilde{h}_2|}{M_1|\tilde{h}_1|}, 1)$, $d^* = \frac{|\tilde{h}_2|}{M_1}$, and $\frac{|\tilde{h}_1|\tilde{w}_1^*}{|\tilde{h}_2|\tilde{w}_2^*} = \frac{1}{M_1}$;
- If $M_1 < \frac{|\tilde{h}_2|}{|\tilde{h}_1|}$, then $(\tilde{w}_1^*, \tilde{w}_2^*) = (1, M_1 \frac{|\tilde{h}_1|}{|\tilde{h}_2|})$, $d^* = |\tilde{h}_1|$, and $\frac{|\tilde{h}_1|\tilde{w}_1^*}{|\tilde{h}_2|\tilde{w}_2^*} = \frac{1}{M_1}$.

From the previous assumption, we know that $\tilde{w}_1 = \sqrt{\frac{2(M_1^2-1)}{3P_1}}w_1$, $\tilde{w}_2 = \sqrt{\frac{2(M_2^2-1)}{3P_2}}w_2$, $|\tilde{h}_1| = \sqrt{\frac{3P_1}{2(M_1^2-1)}}|h_1|$, and $|\tilde{h}_2| = \sqrt{\frac{3P_2}{2(M_2^2-1)}}|h_2|$. After some algebraic manipulations, the conclusion in Theorem 1 can be readily obtained and we complete the proof of the theorem. \square

H. Proof of Corollary 1

Without loss of generality, we consider $\frac{|h_2|}{|h_1|} \leq \sqrt{\frac{P_1(M_2^2-1)}{P_2M_2^2(M_1^2-1)}}$, and therefore $|h_1|w_1^*s_1 + |h_2|w_2^*s_2 = \sqrt{\frac{3P_2M_2^2}{2(M_2^2-1)}}\frac{|h_2|}{|h_1|}|h_1|s_1 + \sqrt{\frac{3P_2}{2(M_2^2-1)}}|h_2|s_2 = \sqrt{\frac{3P_2}{2(M_2^2-1)}}|h_2|(M_2s_1 + s_2)$. Recall that $s_1 \in \mathcal{A}_{M_1} = \{\pm(2k-1)\}_{k=1}^{M_1/2}$ and $s_2 \in \mathcal{A}_{M_2} = \{\pm(2k-1)\}_{k=1}^{M_2/2}$, and therefore $M_2s_1 + s_2 \in \mathcal{A}_{M_1M_2} = \{\pm(2k-1)\}_{k=1}^{M_1M_2/2}$. The quadrature component of the sum-constellation is identical to that of the in-phase component. Hence, the sum-constellation is an $M_1^2M_2^2$ -QAM constellation with a minimum Euclidean distance d_{noma} . The case $\frac{|h_2|}{|h_1|} > \sqrt{\frac{P_1(M_2^2-1)}{P_2M_2^2(M_1^2-1)}}$ can be proved in a similar manner and hence is omitted for brevity. \square

I. Proof of Corollary 2

Recall that d_{noma} and d_{oma} given in (12) and (13), respectively. We consider the following cases one by one as follows:

- 1) If $\frac{M_2^2(M_1^2-1)}{M_2^2-1} \leq \frac{P_1|h_1|^2}{P_2|h_2|^2}$, we have $d_{\text{noma}} = \sqrt{\frac{3P_2}{2(M_2^2-1)}}|h_2|$, and then $\frac{d_{\text{noma}}}{d_{\text{oma},2}} = \sqrt{M_2^2+1} > 1$.
- 2) If $\frac{M_2^2(M_1^2-1)}{M_1^2(M_2^2-1)} \leq \frac{P_1|h_1|^2}{P_2|h_2|^2} < \frac{M_2^2(M_1^2-1)}{M_2^2-1}$, we attain $d_{\text{noma}} = \sqrt{\frac{3P_1}{2M_2^2(M_1^2-1)}}|h_1|$ and then we consider the following two scenarios: (a) For $M_2 \leq M_1$, we conclude $\frac{d_{\text{noma}}}{d_{\text{oma},1}} = \sqrt{\frac{M_1^2+1}{M_2^2}} > 1$; (b) For $M_2 > M_1$, we attain $\frac{d_{\text{noma}}}{d_{\text{oma},2}} = \sqrt{\frac{P_1|h_1|^2(M_2^4-1)}{P_2|h_2|^2M_2^2(M_1^2-1)}}$. As $\frac{P_1|h_1|^2}{P_2|h_2|^2} \geq \frac{M_2^2(M_1^2-1)}{M_1^2(M_2^2-1)}$, we attain $\frac{d_{\text{noma}}}{d_{\text{oma},2}} \geq \sqrt{\frac{M_2^2+1}{M_1^2}} > 1$.
- 3) If $\frac{M_2^2-1}{M_1^2(M_2^2-1)} \leq \frac{P_1|h_1|^2}{P_2|h_2|^2} < \frac{M_2^2(M_1^2-1)}{M_1^2(M_2^2-1)}$, we have $d_{\text{noma}} = \sqrt{\frac{3P_2|h_2|^2}{2M_1^2(M_2^2-1)}}$. Likewise, we consider the following two scenarios: (a) For $M_1 \leq M_2$, then $\frac{d_{\text{noma}}}{d_{\text{oma},2}} = \sqrt{\frac{M_2^2+1}{M_1^2}} > 1$. (b) For $M_1 > M_2$, then $\frac{d_{\text{noma}}}{d_{\text{oma},1}} = \sqrt{\frac{P_2|h_2|^2(M_1^4-1)}{P_1|h_1|^2M_1^2(M_2^2-1)}}$. As $\frac{P_1|h_1|^2}{P_2|h_2|^2} < \frac{M_2^2(M_1^2-1)}{M_1^2(M_2^2-1)}$, we have $\frac{d_{\text{noma}}}{d_{\text{oma},1}} > \sqrt{\frac{M_1^2+1}{M_2^2}} > 1$.
- 4) If $\frac{P_1|h_1|^2}{P_2|h_2|^2} < \frac{M_1^2-1}{M_1^2(M_2^2-1)}$, we attain $\sqrt{\frac{3P_1}{2(M_1^2-1)}}|h_1|$, and hence $\frac{d_{\text{noma}}}{d_{\text{oma},1}} = \sqrt{M_1^2+1} > 1$.

From the above discussion, we can conclude that $d_{\text{noma}} > d_{\text{oma}}$ and this completes the proof. \square

REFERENCES

- [1] H. Tullberg, P. Popovski, Z. Li, M. A. Uusitalo, A. Hoglund, O. Bulacki, M. Fallgren, and J. F. Monserrat, "The METIS 5G system concept: Meeting the 5G requirements," *IEEE Commun. Mag.*, vol. 54, pp. 132–139, Dec. 2016.
- [2] S. Y. Lien, S. L. Shieh, Y. Huang, B. Su, Y. L. Hsu, and H. Y. Wei, "5G new radio: Waveform, frame structure, multiple access, and initial access," *IEEE Commun. Mag.*, vol. 55, no. 6, pp. 64–71, 2017.

- [3] L. Dai, B. Wang, Y. Yuan, S. Han, C. I. I, and Z. Wang, "Non-orthogonal multiple access for 5G: solutions, challenges, opportunities, and future research trends," *IEEE Commun. Mag.*, vol. 53, pp. 74–81, Sept. 2015.
- [4] Z. Ding, Y. Liu, J. Choi, Q. Sun, M. Elkashlan, C. L. I, and H. V. Poor, "Application of non-orthogonal multiple access in LTE and 5G networks," *IEEE Commun. Mag.*, vol. 55, pp. 185–191, Feb. 2017.
- [5] Z. Ding, X. Lei, G. K. Karagiannidis, R. Schober, J. Yuan, and V. Bhargava, "A survey on non-orthogonal multiple access for 5G networks: Research challenges and future trends," *IEEE J. Sel. Areas Commun.*, vol. PP, no. 99, pp. 1–1, 2017.
- [6] P. Wang, J. Xiao, and L. P, "Comparison of orthogonal and non-orthogonal approaches to future wireless cellular systems," *IEEE Veh. Technol. Mag.*, vol. 1, pp. 4–11, Sept. 2006.
- [7] Q. C. Li, H. Niu, A. T. Papathanassiou, and G. Wu, "5G network capacity: Key elements and technologies," *IEEE Veh. Technol. Mag.*, vol. 9, pp. 71–78, Mar. 2014.
- [8] A. Goldsmith, *Wireless Communications*. Cambridge University Press, 2005.
- [9] T. M. Cover and J. A. Thomas, *Elements of Information Theory*. Wiley-Interscience, 2nd ed., 2006.
- [10] A. E. Gamal and Y.-H. Kim, *Network Information Theory*. Cambridge Univ. Press, 2012.
- [11] T. Cover, "Broadcast channels," *IEEE Trans. Inf. Theory*, vol. 18, pp. 2–14, Jan. 1972.
- [12] P. Bergmans, "Random coding theorem for broadcast channels with degraded components," *IEEE Trans. Inf. Theory*, vol. 19, pp. 197–207, Mar. 1973.
- [13] T. Cover, "Comments on broadcast channels," *IRE Trans. Inf. Theory*, vol. 44, pp. 2524–2530, Oct. 1998.
- [14] G. Caire and S. Shamai, "On the achievable throughput of a multiantenna Gaussian broadcast channel," *IEEE Trans. Inf. Theory*, vol. 49, pp. 1691–1706, July 2003.
- [15] D. Slepian and J. K. Wolf, "A coding theorem for multiple access channels with correlated sources," *Bell Syst. Tech. J.*, vol. 52, pp. 1037–1076, Sept. 1973.
- [16] R. S. Cheng and S. Verdú, "Gaussian multiaccess channels with ISI: capacity region and multiuser water-filling," *IEEE Trans. Inf. Theory*, vol. 39, pp. 773–785, May 1993.
- [17] D. N. C. Tse and S. V. Hanly, "Multiaccess fading channels. I. polymatroid structure, optimal resource allocation and throughput capacities," *IEEE Trans. Inf. Theory*, vol. 44, pp. 2796–2815, Nov. 1998.
- [18] S. V. Hanly and D. N. C. Tse, "Multiaccess fading channels. II. delay-limited capacities," *IEEE Trans. Inf. Theory*, vol. 44, pp. 2816–2831, Nov 1998.
- [19] A. Carleial, "A case where interference does not reduce capacity," *IEEE Trans. Inf. Theory*, vol. 21, pp. 569–570, Sept. 1975.
- [20] A. Carleial, "Interference channels," *IEEE Trans. Inf. Theory*, vol. 24, pp. 60–70, Jan. 1978.
- [21] T. S. Han and K. Kobayashi, "A new achievable rate region for the interference channel," *IEEE Trans. Inf. Theory*, vol. 27, pp. 49–60, Jan. 1981.
- [22] A. Wyner, "Recent results in the shannon theory," *IEEE Trans. Inf. Theory*, vol. 20, pp. 2–10, Jan. 1974.
- [23] E. van der Meulen, "A survey of multi-way channels in information theory: 1961-1976," *IEEE Trans. Inf. Theory*, vol. 23, pp. 1–37, Jan. 1977.
- [24] Z. Ding, P. Fan, and H. V. Poor, "Impact of user pairing on 5G nonorthogonal multiple-access downlink transmissions," *IEEE Trans. Veh. Technol.*, vol. 65, pp. 6010–6023, Aug. 2016.
- [25] Y. Liu, Z. Ding, M. Elkashlan, and J. Yuan, "Nonorthogonal multiple access in large-scale underlay cognitive radio networks," *IEEE Trans. Veh. Technol.*, vol. 65, pp. 10152–10157, Dec. 2016.
- [26] Z. Ding, M. Peng, and H. V. Poor, "Cooperative non-orthogonal multiple access in 5G systems," *IEEE Commun. Lett.*, vol. 19, pp. 1462–1465, Aug. 2015.

- [27] Z. Ding, H. Dai, and H. V. Poor, "Relay selection for cooperative NOMA," *IEEE Wireless Commun. Lett.*, vol. 5, pp. 416–419, Aug. 2016.
- [28] Z. Ding, Z. Yang, P. Fan, and H. V. Poor, "On the performance of non-orthogonal multiple access in 5G systems with randomly deployed users," *IEEE Signal Process. Lett.*, vol. 21, pp. 1501–1505, Dec. 2014.
- [29] N. Zhang, J. Wang, G. Kang, and Y. Liu, "Uplink nonorthogonal multiple access in 5G systems," *IEEE Commun. Lett.*, vol. 20, pp. 458–461, Mar. 2016.
- [30] Y. Saito, A. Benjebbour, Y. Kishiyama, and T. Nakamura, "System-level performance evaluation of downlink non-orthogonal multiple access (NOMA)," in *Proc. IEEE Personal Indoor and Mobile Radio Commun. (PIMRC'13)*, pp. 611–615, Sept. 2013.
- [31] Y. Saito, Y. Kishiyama, A. Benjebbour, T. Nakamura, A. Li, and K. Higuchi, "Non-orthogonal multiple access (NOMA) for cellular future radio access," in *Proc. IEEE 77th Vehi. Tech. Conf. (VTC Spring'13)*, pp. 1–5, June 2013.
- [32] A. Benjebbour, A. Li, Y. Saito, Y. Kishiyama, A. Harada, and T. Nakamura, "System-level performance of downlink NOMA for future LTE enhancements," in *Proc. Globecom Workshops (GC Wkshps'13)*, pp. 66–70, Dec. 2013.
- [33] Z. Ding, L. Dai, and H. V. Poor, "MIMO-NOMA design for small packet transmission in the Internet of things," *IEEE Access*, vol. 4, pp. 1393–1405, 2016.
- [34] Z. Dong, Y. Y. Zhang, J. K. Zhang, and X. C. Gao, "Quadrature amplitude modulation division for multiuser MISO broadcast channels," *IEEE J. Sel. Topics Signal Process.*, vol. 10, pp. 1551–1566, Dec. 2016.
- [35] W. Shin, M. Vaezi, B. Lee, D. J. Love, J. Lee, and H. V. Poor, "Non-orthogonal multiple access in multi-cell networks: Theory, performance, and practical challenges," *CoRR*, vol. abs/1611.01607, 2016.
- [36] Z. Dong, H. Chen, J. K. Zhang, and L. Huang, "On non-orthogonal multiple access with finite-alphabet inputs in Z-channels," *IEEE J. Sel. Areas Commun.*, no. 99, 2017.
- [37] 3rd Generation Partnership Project (3GPP), "Study on downlink multiuser superposition transmission (MUST) for LTE (release 13)," *3GPP TR 36.859 V13.0.0*, Dec. 2015.
- [38] H. Lee, S. Kim, and J. H. Lim, "Multiuser superposition transmission (MUST) for LTE-A systems," in *Proc. IEEE Int. Conf. Commun. (ICC'16)*, pp. 1–6, May 2016.
- [39] A. Lozano, A. M. Tulino, and S. Verdu, "Optimum power allocation for parallel Gaussian channels with arbitrary input distributions," *IEEE Trans. Inf. Theory*, vol. 52, pp. 3033–3051, July 2006.
- [40] J. Harshan and B. Rajan, "On two-user Gaussian multiple access channels with finite input constellations," *IEEE Trans. Inf. Theory*, vol. 57, pp. 1299–1327, Mar. 2011.
- [41] J. Harshan and B. S. Rajan, "A novel power allocation scheme for two-user GMAC with finite input constellations," *IEEE Trans. Wireless Commun.*, vol. 12, pp. 818–827, Feb. 2013.
- [42] Y. Wu, C. K. Wen, C. Xiao, X. Gao, and R. Schober, "Linear precoding for the MIMO multiple access channel with finite alphabet inputs and statistical CSI," *IEEE Trans. Wireless Commun.*, vol. 14, pp. 983–997, Feb 2015.
- [43] S. L. Shieh and Y. C. Huang, "A simple scheme for realizing the promised gains of downlink nonorthogonal multiple access," *IEEE Trans. Commun.*, vol. 64, pp. 1624–1635, April 2016.
- [44] A. Dytso, D. Tuninetti, and N. Devroye, "On the two-user interference channel with lack of knowledge of the interference codebook at one receiver," *IEEE Trans. Inf. Theory*, vol. 61, pp. 1257–1276, Mar. 2015.
- [45] T. Kasami and S. Lin, "Coding for a multiple-access channel," *IEEE Trans. Inf. Theory*, vol. 22, pp. 129–137, Mar. 1976.
- [46] T. Kasami and S. Lin, "Bounds on the achievable rates of block coding for a memoryless multiple-access channel," *IEEE Trans. Inf. Theory*, vol. 24, pp. 187–197, Mar. 1978.
- [47] R. Ahlswede and V. Balakirsky, "Construction of uniquely decodable codes for the two-user binary adder channel," *IEEE Trans. Inf. Theory*, vol. 45, pp. 326–330, Jan. 1999.

- [48] M. Al-Imari, P. Xiao, M. A. Imran, and R. Tafazolli, "Uplink non-orthogonal multiple access for 5G wireless networks," in *n Proc. 11th Int. Symp. on Wireless Commun. Syst. (ISWCS'14)*, pp. 781–785, Aug. 2014.
- [49] X. Xiao, Q. Huang, and E. Viterbo, "Joint optimization scheme and sum constellation distribution for multi-user Gaussian multiple access channels with finite input constellations," in *Proc. 2016 Australian Commu. Theory Workshop (AusCTW)*, pp. 130–135, Jan. 2016.
- [50] G. Hardy and E. Wright, *An Introduction to the Theory of Numbers*. Oxford Univ. Press, 4 ed., 1975.
- [51] S. Lagen, A. Agustin, and J. Vidal, "On the superiority of improper Gaussian signaling in wireless interference MIMO scenarios," *IEEE Trans. Commun.*, vol. 64, pp. 3350–3368, Aug. 2016.
- [52] V. R. Cadambe, S. A. Jafar, and C. Wang, "Interference alignment with asymmetric complex signaling: Settling the Høst-Madsen-Nosratinia conjecture," *IEEE Trans. Inf. Theory*, vol. 56, pp. 4552–4565, Sept. 2010.
- [53] V. R. Cadambe and S. A. Jafar, "Interference alignment and degrees of freedom of the K -user interference channel," *IEEE Trans. Inf. Theory*, vol. 54, pp. 3425–3441, Aug. 2008.
- [54] R. H. Etkin, D. Tse, and H. Wang, "Gaussian interference channel capacity to within one bit," *IEEE Trans. Inf. Theory*, vol. 54, pp. 5534–5562, Dec. 2008.
- [55] G. Bresler, A. Parekh, and D. Tse, "The approximate capacity of the many-to-one and one-to-many Gaussian interference channels," *IEEE Trans. Inf. Theory*, vol. 56, pp. 4566–4592, Sept. 2010.
- [56] R. Prasad, S. Bhashyam, and A. Chockalingam, "On the Gaussian many-to-one X channel," *IEEE Trans. Inf. Theory*, vol. 62, pp. 244–259, Jan. 2016.
- [57] M. Zeng, A. Yadav, O. A. Dobre, G. I. Tsiropoulos, and H. V. Poor, "Capacity comparison between MIMO-NOMA and MIMO-OMA with multiple users in a cluster," *IEEE J. Sel. Areas Commun.*, vol. PP, no. 99, pp. 1–1, 2017.
- [58] A. S. Avestimehr, S. N. Diggavi, and D. Tse, "Wireless network information flow: A deterministic approach," *IEEE Trans. Inf. Theory*, vol. 57, pp. 1872–1905, Apr. 2011.